



HAL
open science

Plutonium isotopic signatures in soils and their variation (2011-2014) in sediment transiting a coastal river in the Fukushima Prefecture, Japan

Hugo Jaegler, Fabien Pointurier, Yuichi Onda, Amélie Hubert, J. Patrick Laceby, Maëva Cirella, O. Evrard

► To cite this version:

Hugo Jaegler, Fabien Pointurier, Yuichi Onda, Amélie Hubert, J. Patrick Laceby, et al.. Plutonium isotopic signatures in soils and their variation (2011-2014) in sediment transiting a coastal river in the Fukushima Prefecture, Japan. *Environmental Pollution*, 2018, 240, pp.167-176. 10.1016/j.envpol.2018.04.094 . cea-02610576

HAL Id: cea-02610576

<https://cea.hal.science/cea-02610576>

Submitted on 18 May 2020

HAL is a multi-disciplinary open access archive for the deposit and dissemination of scientific research documents, whether they are published or not. The documents may come from teaching and research institutions in France or abroad, or from public or private research centers.

L'archive ouverte pluridisciplinaire **HAL**, est destinée au dépôt et à la diffusion de documents scientifiques de niveau recherche, publiés ou non, émanant des établissements d'enseignement et de recherche français ou étrangers, des laboratoires publics ou privés.

1 **Plutonium isotopic signatures in soils and their variation (2011-2014) in**
2 **sediment transiting a coastal river in the Fukushima Prefecture, Japan**
3

4 Hugo Jaegler¹, Fabien Pointurier², Yuichi Onda³, Amélie Hubert², J. Patrick Lacey^{1,4},
5 Maëva Cirella² & Olivier Evrard^{1*}

6

7 **Affiliations**

8 ¹Laboratoire des Sciences du Climat et de l'Environnement, LSCE/IPSL, Unité Mixte de Recherche 8212 (CEA-
9 CNRS-UVSQ), Université Paris-Saclay, F-91198 Gif-sur-Yvette, France

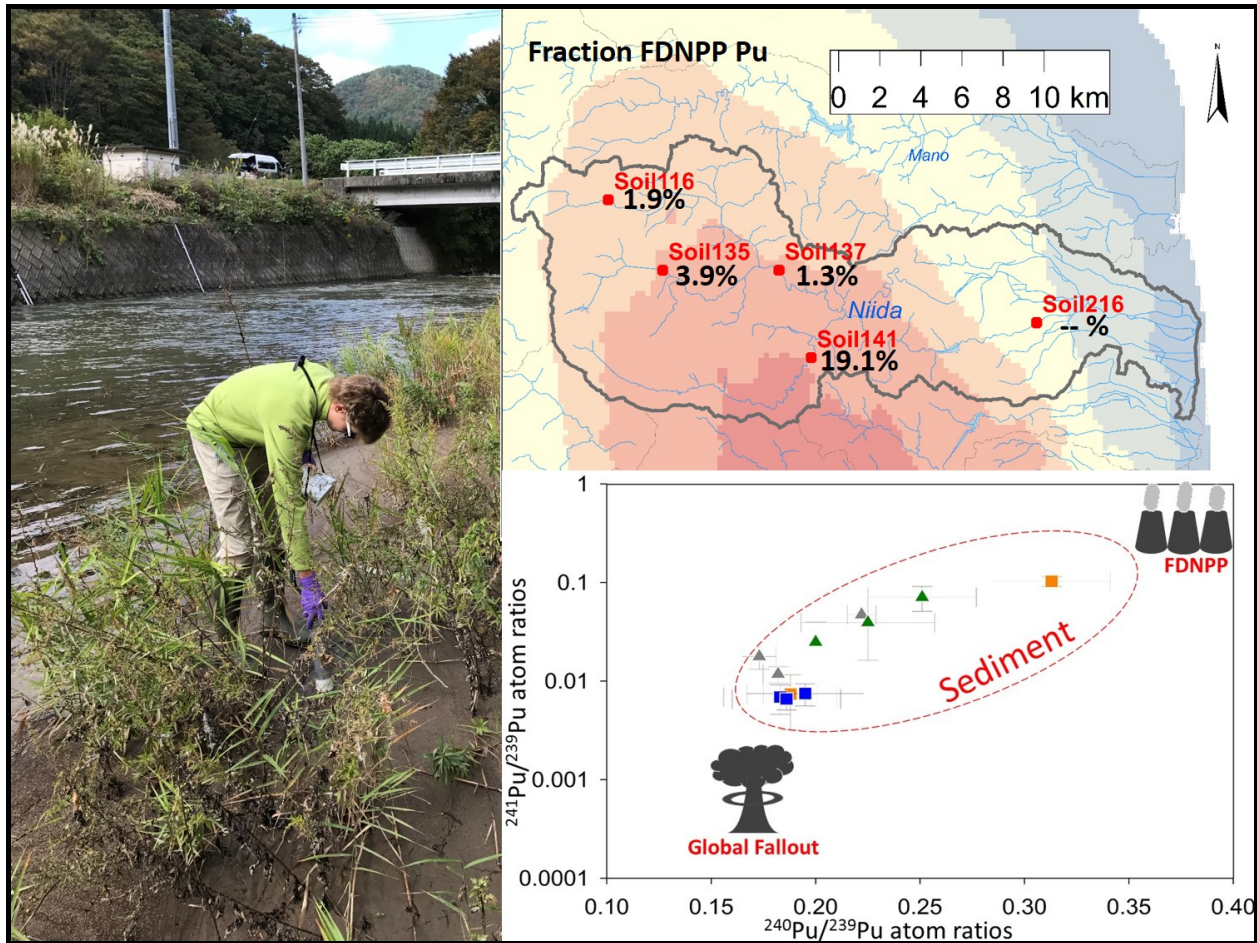
10 ²CEA, DAM, DIF, F-91297 Arpajon, France

11 ³Center for Research in Isotopes and Environmental Dynamics (CRIED), University of Tsukuba, Tsukuba,
12 Japan

13 ⁴Environmental Monitoring and Science Division, Alberta Environment and Parks, 3115 - 12 Street NE
14 Calgary, Alberta, Canada

15 (*) Corresponding author (email address: olivier.evrard@lscce.ipsl.fr).

16 Graphical abstract



17

18 **Abstract**

19 The Fukushima Daiichi Nuclear Power Plant (FDNPP) accident resulted in a significant release of
20 radionuclides that were deposited on soils in Northeastern Japan. Plutonium was detected at trace levels
21 in soils and sediments collected around the FDNPP. However, little is known regarding the spatial-
22 temporal variation of plutonium in sediment transiting rivers in the region. In this study, plutonium
23 isotopic compositions were first measured in soils (n=5) in order to investigate the initial plutonium
24 deposition. Then, plutonium isotopic compositions were measured on flood sediment deposits (n=12)
25 collected after major typhoon events in 2011, 2013 and 2014. **After a thorough radiochemical**
26 purification, isotopic ratios ($^{240}\text{Pu}/^{239}\text{Pu}$, $^{241}\text{Pu}/^{239}\text{Pu}$ and $^{242}\text{Pu}/^{239}\text{Pu}$) were measured with a Multi-
27 Collector Inductively Coupled Mass Spectrometer (MC ICP-MS), providing discrimination between
28 plutonium derived from global fallout, from atmospheric nuclear weapon tests, and plutonium derived
29 from the FDNPP accident. Results demonstrate that soils with the most Fukushima-derived plutonium
30 were in the main radiocaesium plume and that there was a variable mixture of plutonium sources in the

31 flood sediment samples. Plutonium concentrations and isotopic ratios generally decreased between
32 2011 and 2014, reflecting the progressive erosion and transport of contaminated sediment in this coastal
33 river during flood events. Exceptions to this general trend were attributed to the occurrence of
34 decontamination works or the remobilisation of contaminated material during typhoons. The different
35 plutonium concentrations and isotopic ratios obtained on three aliquots of a single sample suggest that
36 the Fukushima-derived plutonium was likely borne by discrete plutonium-containing particles. In the
37 future, these particles should be isolated and further characterized in order to better understand the
38 fate of this long-lived radionuclide in the environment.

39 **Capsule**

40 Plutonium concentrations and isotopic ratios in sediment transiting a river draining the main Fukushima
41 radioactive pollution plume decreased with time.

42 **Keywords**

43 FDNPP accident; river lag deposits; Multi Collector-Inductively Coupled Plasma-Mass Spectrometer;
44 Actinide; Pu atom ratios; Source identification

45 **Highlights**

- 46 • Measurement of Pu in soil and river sediment by MC ICP-MS.
- 47 • Determination of Pu sources by isotopic composition.
- 48 • FDNPP-derived Pu deposition was heterogeneous in the environment.
- 49 • Pu contribution from FDNPP accident varied between 1.1–39.2% of total plutonium.
- 50 • Variability of concentrations suggests the occurrence of discrete Pu-bearing particles.

51

52 **Introduction**

53 The 2011 Fukushima Dai-ichi Nuclear Power Plant (FDNPP) accident released significant quantities of
54 radioactive contamination into the environment. Although ~80% of the atmospheric fallout from the
55 accident occurred over the ocean, the remainder was deposited on Japanese soils and formed a major
56 radioactive pollution plume extending ~70 km northwest of the FDNPP (Evrard et al., 2015; Kawamura et
57 al., 2011). Most of the research conducted after the accident has focused on gaseous radionuclides or
58 radiocaesium isotopes (Bailly du Bois et al., 2012; Estournel et al., 2012; TEPCO, 2012). Other
59 radionuclides, such as plutonium isotopes were also studied, although to a lesser extent (Steinhauser,
60 2014).

61 Plutonium is present in the Northern Hemisphere environment as a result of nuclear weapon tests
62 ([Yamamoto et al., 2014](#)). ^{239}Pu ($T_{1/2}=24,110$ y, alpha-decay) and ^{240}Pu ($T_{1/2}=6,563$ y, alpha-decay) are the
63 most abundant isotopes in the environment on a global scale, while ^{238}Pu ($T_{1/2}=88.74$ y, alpha-decay),
64 ^{241}Pu ($T_{1/2}=14.35$ y, beta-decay) and ^{242}Pu ($T_{1/2}=376,000$ y, alpha-decay) are present in smaller
65 concentrations ([Hardy et al., 1973](#); [Harley, 1979](#); [Kelley et al., 1999](#); [Yang et al., 2015](#)). As the isotopic
66 composition of plutonium is related to its origin, these isotopic ratios provide a powerful tool to
67 discriminate between different sources of plutonium in the environment ([Muramatsu et al., 2003](#)).
68 Specific isotopic signatures have been reported for the global fallout associated with nuclear weapon
69 testing, local nuclear weapon tests ([Chiappini et al., 1999](#)), the Chernobyl accident ([Ketterer et al., 2004](#))
70 and the FDNPP accident ([Evrard et al., 2014b](#)).

71 Plutonium concentrations associated with the global fallout were shown to be heterogeneous in
72 different aliquots ([Kelley et al., 1999](#)), due to the particulate form of deposition ([Salbu, 2011](#)).
73 Contamination from the global fallout and the FDNPP have very different origins and their
74 concentrations may change differently with time: global fallout contamination originated from the
75 stratosphere, with many episodes spread over several decades, whereas FDNPP was supplied by a single
76 local source at a much lower altitude, during a few days only. In contrast, plutonium isotopic ratios
77 associated with the global fallout are homogeneous ([Kelley et al., 1999](#)) and $^{241}\text{Pu}/^{239}\text{Pu}$ isotopic ratios
78 may be used in particular to calculate the respective plutonium concentrations originating from the
79 FDNPP accident or the global fallout. Due to the relative short half-life of ^{241}Pu (14.35 y), the global
80 fallout source of this isotope has decayed significantly, whereas plutonium released by the FDNPP
81 accident contains abundant levels of ^{241}Pu (1.1×10^{11} - 2.6×10^{11} Bq, ([Zheng et al., 2012b](#))). Its detection in
82 the environment therefore provides unambiguous evidence of the FDNPP release. ([Evrard et al., 2014b](#)).

83 The plutonium isotopic composition in the fuel from the FDNPP was reconstructed at the moment of the
84 accident based on simulations ([Kirchner et al., 2012](#); [Nishihara et al., 2012](#); [Schwantes et al., 2012](#)) (Table
85 1). The global fallout atom ratios were also quantified ([Kelley et al., 1999](#); [Muramatsu et al., 2003](#); [Yang
86 et al., 2015](#); [Zhang et al., 2010](#)) (Table 1). The fate of FDNPP-derived plutonium can therefore be
87 investigated in the environment based on $^{240}\text{Pu}/^{239}\text{Pu}$, $^{241}\text{Pu}/^{239}\text{Pu}$ and $^{242}\text{Pu}/^{239}\text{Pu}$ isotopic ratios as
88 demonstrated by Evrard *et al.* ([2014b](#)).

89 Zheng *et al.* ([2013](#)) published a comprehensive review of plutonium releases from the FDNPP accident.
90 Since then, additional measurements reported by various authors on litter, soil, and river water samples
91 collected in the Fukushima Prefecture after the accident indicated that some environmental samples

92 contained plutonium from the FDNPP reactors ([Kimura et al., 2015](#); [Utsunomiya et al., 2012](#); [Xu et al.,](#)
93 [2016](#)) (Table S1, Figure 1). However, these studies were mainly based on measurements by alpha-
94 spectrometry of the $^{239+240}\text{Pu}$ and ^{238}Pu activities and of the $^{238}\text{Pu}/^{239+240}\text{Pu}$ isotopic ratio. Using alpha-
95 spectrometry, FDNPP-derived plutonium was detected only in a few samples located near the plant,
96 because alpha-spectrometry lacks in sensitivity and energy resolution to measure the $^{240}\text{Pu}/^{239}\text{Pu}$ isotopic
97 ratio. As a beta-emitter, ^{241}Pu is not measurable by alpha-spectrometry and its analysis by beta-
98 spectrometry has relatively poor detection limits (minimum of 10 mBq) ([Rosner et al., 1992](#)) compared
99 to those obtained by mass spectrometry. ^{242}Pu has a very long half-life and cannot be measured
100 efficiently by alpha-spectrometry at the ultra-trace level. Finally, ^{242}Pu is often used as an isotope dilution
101 tracer for alpha spectrometry measurements.

102 In contrast, all plutonium isotopes, with the exception of ^{238}Pu (because of the presence of ^{238}U
103 isotopes), can be measured by Inductively Coupled Plasma Mass Spectrometry (ICP-MS) with high
104 accuracy. As mentioned in the literature review by Zheng *et al.* ([2013](#)), and summarized in Table S1 and
105 Figure 1, ^{241}Pu and ^{242}Pu were only measured in a few studies, even though these isotopes are powerful
106 tracers for identifying different sources of plutonium.

107 The objective of this current research was therefore to investigate the temporal variations of plutonium
108 contamination in **flood** sediment in order to improve our understanding of plutonium dynamics in the
109 FDNPP fallout-impacted region. As plutonium is strongly bound to the fine sediment mineral fraction
110 ([Kersting, 2013](#); [Meusburger et al., 2016](#)), plutonium may be eroded, deposited and remobilised during
111 rainfall events ([Ministry of Land Infrastructure and Transport, 2006](#); [Yoshimura et al., 2005](#)). In the
112 Fukushima Prefecture, soil erosion and sediment transport were shown to be exacerbated during the
113 typhoon season ([Chartin et al., 2013](#); [Evrard et al., 2013](#); [Yamashiki et al., 2014](#)).

114 Two types of samples were collected and analysed: i) **recently deposited flood sediment** collected at four
115 sampling locations and in three different years to investigate the evolution of plutonium concentration
116 and composition in a coastal catchment of the Fukushima Prefecture; and ii) soil samples collected at five
117 sampling locations across the main radioactive plume to characterize the initial deposition of FDNPP-
118 originating plutonium and compare its spatial pattern with that of the well-documented radiocaesium
119 contamination plume ([Chartin et al., 2013](#)). To the best of our knowledge, this study represents the first
120 attempt to characterise variations of plutonium contamination in sediment transiting a coastal river
121 system draining the main radioactive plume in the Fukushima Prefecture.

122

123 **Methodology**

124 ***Study Area and Sampling***

125 The main radioactive plume drained by Fukushima coastal rivers to the Pacific Ocean is located in the
126 upper areas of these catchments (Figure 1). Contaminated sediment may therefore be eroded and
127 transported to the coastal plains that were exposed to lower initial fallout levels. However, sediment was
128 shown to be trapped in dams and reservoirs ([Lepage et al., 2016](#)), which delays their progressive transfer
129 from contaminated upper catchment areas to the Pacific Ocean. Accordingly, this study will examine
130 plutonium isotopic ratios in samples (including river sediment and soils) collected at different locations
131 along the Niida River, where the only dam is located on a tributary and will therefore have a limited
132 impact on sediment transport in this catchment ([Lepage et al., 2016](#)).

133 The Niida catchment (271 km²) is mainly covered with forests (75%), cultivated (12%) and built-up areas
134 (22%) found in river valleys ([Evrard et al., 2016](#)). The soil sampling locations are located along the Niida
135 River, in zones characterised by different levels of initial radiocaesium contamination (Figure 1).

136 **The soil samples (top 1-2 cm) were collected in April 2012 and November 2012 (Figure 1, Table S2),**
137 **following the protocol described elsewhere ([Lacey et al., 2016b](#)). In brief, soil was taken with a small**
138 **plastic trowel and composed by 10 scrape subsamples. These subsamples were well mixed in the bag**
139 **used to collect them.** One sample was collected in the area characterised by the highest radiocaesium
140 contamination (FSN 141). Three samples (FNS 116, FNS 135 and FNS 137) were taken in the moderate
141 contaminated zone in the upper part of the catchment. The last sample (FNS 216) was collected in the
142 less contaminated zone, in the downstream part of the catchment (Table S2).

143 The **flood** sediment sampling locations include two sites in the upper catchment (“Upstream Zone 1” and
144 “Upstream Zone 2”), and two sites downstream (“Downstream Zone 1” and “Downstream Zone 2”)
145 (Figure 1). GPS coordinates of the sampling locations are provided in Table S2. River sediment samples
146 were taken from material deposited after typhoons at these sites in November 2011, November 2013
147 and November 2014. These lag deposit samples correspond to fine particulate material that settled on
148 channel banks, inset benches and floodplains. **Care was taken to sample the fine material with a trowel**
149 **or, when those deposits were too thin, with a spatula (down to the underlying coarser material layer).**
150 **These recent flood deposits have proven to be comparable to in-situ suspended sediment samples in**
151 **recent research conducted in similar erosive environments ([Lal et al., 2015](#); [Olley et al., 2013](#)).** Each
152 sample was composed of at least 5 subsamples collected over a 5 m reach using a plastic trowel. **The**

153 homogeneity of the radiocesium contamination across these river sections was verified in the field
154 through the measurement of radiation rates using a radiameter on recent drape deposits in a 10 to 20 m
155 wide area along rivers (Evrard et al., 2014a; Evrard et al., 2013). For the Downstream Zone 2 sampling
156 point, located near the estuary of the Niida River, flood sediment was sampled on the alluvial plain
157 terrace that is not subject to daily tides in order to limit the potential impact of seawater plutonium (Bu
158 et al., 2014). The potential heterogeneity of plutonium deposition was investigated by subdividing one
159 sample (FNL 492) into three aliquots, which were measured for plutonium isotopic ratios and
160 concentrations with the same protocol as the other samples.

161 **Sample preparation**

162 For each chemical preparation, 3 process blanks were prepared with the samples. Sample preparation
163 (i.e. dissolution, separation and purification) is described in detail in a previous paper (Evrard et al.,
164 2014b). In summary, samples were well mixed, dried in the oven at 40°C for 72 h and sieved to 2 mm.
165 Then they were ground to a fine powder using an agar mortar and stored at room temperature before
166 analysis. A ~5 g aliquot was transferred to a Pyrex beaker, covered with watch glasses and reduced to
167 ash at 450°C for ~15 h in an electric furnace to decompose organic matter. After cooling to room
168 temperature, in order to avoid interferences of isotopic impurities, a limited amount of ~100 fg of ²⁴⁴Pu
169 (diluted solution prepared from certified isotopic reference material IRMM-042a, Geel, Belgium) was
170 added to the samples as an isotopic dilution tracer. Ashes were leached with concentrated HNO₃ (50
171 mL), evaporated to dryness, leached again with aqua regia (50 mL), evaporated to dryness, leached again
172 with concentrated HCl (50 mL), evaporated to dryness, recovered with 2 M HCl and then filtered with a
173 disposable 0.45 µm Nalgene filtering unit (Thermo Scientific, Rochester, NY, USA). The dissolved fraction
174 was evaporated to dryness and recovered with concentrated HNO₃ (30 mL). A few mg of NaNO₂ were
175 added to adjust and stabilize the redox state of plutonium at (+IV). After evaporation, 30 mL of 8 M HNO₃
176 were added to the sample prior to its loading onto a preconditioned ion-exchange resin column for
177 plutonium purification.

178 Plutonium was first purified with a Dowex AG1X8 anion exchange resin filled with ~10 mL of 50-100
179 mesh AG1X8 resin then ~10 mL of 100-200 mesh AG1X8 resin, rinsed twice and conditioned with 8 M
180 NHO₃. After loading the sample solution onto the column, the resin was washed with 8 M HNO₃ (U-Am
181 fraction elution), 10 M HCl (Th fraction elution) and NH₄I (1.5%) – 12 M HCl to elute plutonium from the
182 resin. A second purification was performed with a Dowex AG1X4 anion-exchange resin (100-200 mesh
183 resin), with the same wash operations and elution solution. Ion-exchange resins were used to purify and

184 concentrate plutonium from other potentially interfering elements (mainly U, Am and Pb). The final
185 eluting solution was evaporated to dryness several times and recovered with concentrated HNO₃ to
186 eliminate chloride. The last recovery was achieved with 3 mL of 2% HNO₃ for ICP-MS measurements.
187 Overall, mean plutonium recovery was 72% (range: 39-83%, standard deviation: 14%). Plutonium
188 purification used Dowex resins to completely remove ²⁴¹Am (>99%), which may interfere with the
189 detection of ²⁴¹Pu by ICP-MS. As a trivalent ion, americium is not retained by the Dowex AG1X8 resin in
190 nitric acid ([Trémillon, 1965](#)) (i.e. during the introduction of the sample into the column and the following
191 washing step with 8M HNO₃).

192 ***Mass spectrometry for plutonium atom ratio and concentration measurements***

193 Plutonium isotopic composition and concentrations were measured with a Multi-Collector ICP-MS (MC
194 ICP-MS) (“Neptune Plus”, Thermo-Fisher-Scientific., Bremen, Germany). The instrument was equipped
195 with a Desolvating System (Cetac “Aridus II”) and with high-efficiency cones (“Jet-cones”, Thermo-
196 Fischer-Scientific). **Both equipments increased** the sensitivity of the instrument by a factor of ~10. Five
197 ion counters and eight Faraday cups are available for simultaneous measurement of all plutonium
198 isotopes. Multi-collector measurements were performed in the static mode (Table S3).

199 Two certified reference materials were used: IRMM 186 (IRMM, Geel, Belgium) certified for ²³⁴U/²³⁸U,
200 ²³⁵U/²³⁸U and ²³⁶U/²³⁸U isotopic ratios, and IRMM 057 certified for ²³³U concentration used as isotopic
201 dilution tracer for uranium isotope ratio measurements. Mass bias, hydride formation rates, peak tails
202 and gain factors of the ion counters were determined with a 5 ppb U solution of IRMM 186 and a
203 calibrated mixed solution of IRMM 186 and IRMM 057. Both U standard solutions were diluted in 2%
204 HNO₃. Results were systematically corrected for variation of the relative efficiency of the detectors
205 (referred to as “gain factors” of the detectors) with respect to a selected Faraday cup. Relative standard
206 deviations of the gain factors ranged between 0.3% and 5.1% during an analysis. **These correction factors**
207 **were applied to the measurement of a certified plutonium standard (CRM-128) during the analytical**
208 **procedure (n>4), in order to verify the accuracy of the corrections (determined on a uranium standard)**
209 **on plutonium samples.**

210 Mass bias was corrected according to the ²³⁵U/²³⁸U value of the IRMM 186 standard measured before
211 and after each sample analysis and applying an exponential law. Hydride formation rates and the peak
212 tail at mass unit +1 were determined by measuring the (239 atomic mass unit)/²³⁸U ratio in the IRMM
213 186 standard solution (which does not contain plutonium), while the peak tail at mass unit +2 was

214 calculated by measuring the (240 atomic mass unit)/²³⁸U ratio in the same standard solution. **Hydride**
215 **and tail correction factors were systematically determined and applied. However, this correction did not**
216 **exceed 0.4% in those results provided in this manuscript.**

217 Detector configurations for measurements and gain factor calculations are shown in the Supplementary
218 Material. ²⁴⁴Pu tracer isotopic impurities were corrected according to the certificate of the isotopic
219 reference material IRMM-042a. Polyatomic interferences, mainly from PbO₂⁺ and PbAr⁺, were evaluated
220 and corrected by measuring pure mono-elemental solutions of Pb at the end of the procedure. They
221 were corrected through the calculation of their formation ratios and through the measurement of the
222 count rates of Pb in the samples ([Pointurier et al., 2011](#)).

223 Finally, all plutonium isotopic ratios and plutonium concentrations provided in this study were corrected
224 for the average plutonium content of the three chemical blanks. Isotopic ratios were then deduced from
225 these concentrations and decay-corrected to March 15, 2011. Associated uncertainties were propagated
226 during all calculations. Unless otherwise stated, all following uncertainties are expanded with a
227 confidence level of 95% (e.g. a coverage factor of 2).

228 **The validity of the correction method was verified by analysing several certified reference materials.**
229 **IAEA-385 and IAEA-447 are certified for ²³⁹⁺²⁴⁰Pu mass activities. The results of the current research**
230 **remained in good agreement with these certified values (Table S4).** Ultra-traces of plutonium isotopes
231 (mean total plutonium: 0.5 ± 3.4 fg) were detected in the process blanks, and these may originate from
232 the different chemicals used for the additional leaching steps or subsequent contaminations during
233 evaporation steps.

234 ***Protocol validation for plutonium extraction from sediment samples***

235 In the protocol described above, it is assumed that plutonium is entirely extracted from the samples and
236 insoluble fractions were therefore not analysed. In order to validate this assumption (i.e. the
237 effectiveness of this protocol in recovering the plutonium from both global fallout and FDNPP sources
238 from sediment samples) and consequently to evaluate the potential residual plutonium concentration in
239 the insoluble fraction after filtration, an additional treatment was carried out on insoluble fractions to
240 fully dissolve them. In brief, insoluble fractions and chemical blanks were transferred into clean and new
241 Teflon beakers, spiked with ~70 fg of ²⁴²Pu (diluted solution prepared from a certified reference tracer,
242 AEA Technology, UK), and submitted to 4 additional acid leaching steps: 3 with concentrated HF (40%
243 weight) and concentrated HNO₃, and a 4th leaching with concentrated HNO₃ and H₂O₂. After each

244 leaching step, samples were evaporated to dryness on a hot plate (135°C covered with Teflon watch
245 glass). At the end of this additional treatment, all samples were almost entirely dissolved, with the
246 exception of a few refractory particles. A filtration was performed in order to remove the last visible
247 solid residue. After carrying out similar plutonium purification with two Dowex anion exchange resins as
248 for the soluble fraction, plutonium concentrations were measured in both soluble and insoluble fractions
249 (Table S5).

250 Results showed that total plutonium masses in the soluble fractions ($^{239}\text{Pu} + ^{240}\text{Pu} + ^{241}\text{Pu}$) after acid
251 leaching varied between 150 and 370 fg, while the total plutonium masses in the blanks were
252 systematically lower than 2 fg for these measurements. In contrast, plutonium masses in the insoluble
253 fractions ($^{239}\text{Pu} + ^{240}\text{Pu} + ^{241}\text{Pu}$) remained lower than 20 fg, representing less than 5% of the plutonium
254 contained in the soluble fractions. These results confirm the effectiveness of the leaching dissolution
255 protocol, which is sufficient to dissolve and recover a mean of (96 ± 1) % of plutonium contained in the
256 samples.

257 ***FDNPP and global fallout plutonium contributions***

258 The fraction of plutonium in sediment (“sample”) originating from the FDNPP or the global fallout (“GF”) was
259 calculated using a two-source mixing model (Kelley et al., 1999) with the respective isotopic
260 abundances (Ab) of ^{241}Pu in the sample ($\text{Ab}(^{241}\text{Pu})_{\text{sample}}$), in the global fallout ($\text{Ab}(^{241}\text{Pu})_{\text{GF}}$) and at
261 FDNPP ($\text{Ab}(^{241}\text{Pu})_{\text{FDNPP}}$). Isotopic abundances were calculated for each data set: the samples analysed
262 in the current research, global fallout and FDNPP. Each data set corresponds to the isotopic ratios
263 $^{240}\text{Pu}/^{239}\text{Pu}$, $^{241}\text{Pu}/^{239}\text{Pu}$ and $^{242}\text{Pu}/^{239}\text{Pu}$ measured in each sample in the current study (Table 2) or those
264 determined for global fallout and FDNPP signatures and published in the literature (Table 1). $\text{Ab}(^{241}\text{Pu})_i$,
265 where i represented either “sample” or “GF” or “FDNPP”, was calculated using Equation (1):

$$\text{Ab}(^{241}\text{Pu})_i = \frac{(^{241}\text{Pu}/^{239}\text{Pu})_i}{1 + (^{240}\text{Pu}/^{239}\text{Pu})_i + (^{241}\text{Pu}/^{239}\text{Pu})_i + (^{242}\text{Pu}/^{239}\text{Pu})_i} \quad (1)$$

266 where $(^{240}\text{Pu}/^{239}\text{Pu})_i$, $(^{241}\text{Pu}/^{239}\text{Pu})_i$ and $(^{242}\text{Pu}/^{239}\text{Pu})_i$ are atomic ratios.

267 Although plutonium isotopic ratios measured in soils before the FDNPP accident were shown to be
268 rather homogeneous in the environment (Kelley et al., 1999), slight variations in the isotopic signature of
269 plutonium emitted by the global fallout associated with nuclear tests were observed, and were shown to
270 depend on the distance from the nuclear test sites, the proportion of stratospheric debris and their

271 location in the Southern or the Northern Hemisphere ([Evrard et al., 2014b](#)). Kelley *et al.* ([1999](#)), Zhang *et*
272 *al.* ([2010](#)), Yang *et al.* ([2015](#)) and Muramatsu *et al.* ([2003](#)) reported isotopic ratios ($^{240}\text{Pu}/^{239}\text{Pu}$,
273 $^{241}\text{Pu}/^{239}\text{Pu}$ and $^{242}\text{Pu}/^{239}\text{Pu}$) measured in soils collected worldwide before the FDNPP accident (Table 1).
274 Accordingly, the mean of these isotopic ratios was used to characterize the isotopic abundance
275 associated with the global fallout: $\text{Ab}(^{241}\text{Pu})_{\text{GF}} = (1.27 \pm 0.13) \times 10^{-3}$.

276 Nishihara *et al.* ([Nishihara et al., 2012](#)), Kirchner *et al.* ([2012](#)) and Schwantes *et al.* ([2012](#)) estimated with
277 the ORIGEN model the fuel compositions at the FDNPP at the moment of the accident (Table 1). The
278 abundance of ^{241}Pu from the FDNPP was determined using the mean of these isotopic ratios: $\text{Ab}(\text{$
279 $^{241}\text{Pu})_{\text{FDNPP}} = (1.15 \pm 0.12) \times 10^{-1}$.

280 Finally, the fraction of plutonium originating from the FDNPP (X_{FDNPP}), i.e. the proportion of FDNPP-
281 derived plutonium in each sample, was calculated for each sample using $\text{Ab}(^{241}\text{Pu})_{\text{sample}}$, $\text{Ab}(^{241}\text{Pu})_{\text{GF}}$ and
282 $\text{Ab}(^{241}\text{Pu})_{\text{FDNPP}}$ in Equation (2).

$$\text{Ab}(^{241}\text{Pu})_{\text{FDNPP}} \times X_{\text{FDNPP}} + \text{Ab}(^{241}\text{Pu})_{\text{GF}} \times (1 - X_{\text{FDNPP}}) = \text{Ab}(^{241}\text{Pu})_{\text{sample}} \quad (2)$$

283

284 ***Radiocesium measurements and calculation of $^{239+240}\text{Pu}/^{137}\text{Cs}$ activity ratios***

285 ^{137}Cs activities were measured by gamma spectrometry using HPGe detectors (Canberra/Ortec) following
286 the procedure described by [Chartin et al. \(2013\)](#). These ^{137}Cs measurements were used to calculate the
287 $^{239+240}\text{Pu}/^{137}\text{Cs}$ activity ratios. In the literature, this ratio has been used to determine the amount of Pu
288 released during the accident ([Sakaguchi et al., 2014](#); [Zheng et al., 2012b](#)). In the current research, as the
289 contributions of FDNPP-derived plutonium were determined for each sample (Equation 2), the
290 corresponding activities of ^{239}Pu and ^{240}Pu originating from FDNPP were calculated for each individual
291 sample and the $^{239+240}\text{Pu}/^{137}\text{Cs}$ activity ratios were determined with those FDNPP-derived plutonium
292 activities.

293 ***Particulate matter properties and particle size parameters measurements***

294 Particle size of the samples was analysed with laser granulometry (Malvern Mastersizer[®]) characterizing
295 the textural parameters of particles ranging between 0.01 and 3500 μm , and the corresponding median
296 diameters (d50) and Specific Surface Areas (SSA) of sediment samples were calculated. The EA-IRMS
297 analyses were conducted with a continuous flow Elementar[®] VarioPyro cube analyzer coupled to a
298 Micromass[®] Isoprime Isotope Ratio Mass Spectrometer (IRMS). The soil and sediment samples were

299 packed into tin capsules and all samples were first analyzed for Total Organic Carbon (TOC) and $\delta^{13}\text{C}$ using
300 a set of tyrosine standards to calibrate TOC and Total Nitrogen (TN) concentrations and $\delta^{13}\text{C}$
301 measurements. C and $\delta^{13}\text{C}$ content were determined using an online continuous flow elemental analyzer
302 Flash 2000 HT, coupled with an Isotopic Ratio Mass Spectrometer Delta V Advantage via a conflow IV
303 interface from Thermo Fischer Scientific. C quantification was performed using a Certified reference
304 material EMAP 2 purchased from IVA Analysentechnik (%C = 68.35 ± 0.28 %). Isotopic calibration was
305 achieved using a Certified reference material: EMAP2 (-28.19 ± 0.14 ‰), and an Organic Analytical
306 Standard (from Elemental Microanalysis): Sorghum Flour (-13.78 ± 0.17 ‰). In addition, a reference
307 material LOS (Low Organic content Soil standard, from Elemental Microanalysis, %C= 1.61 ± 0.09 %, $\delta^{13}\text{C} = -$
308 26.66 ± 0.24 ‰) was used to assess the accuracy and reproducibility during the run. The standard deviation
309 for LOS C content was of 1.65 ± 0.11 % (n=3). For $\delta^{13}\text{C}$ values, the standard deviation during the entire run
310 was of 0.09 ‰ (n=8) for EMAP2, 0.29 ‰ (n=8) for Sorghum, and 0.21 ‰ (n=3) for LOS.

311 **Results and Discussion**

312 ***Pu isotopic measurements***

313 Plutonium isotopic atom ratios and plutonium mass concentrations (fg of total plutonium per g of dry
314 sediment) are provided in Table 2, while temporal variations of $^{240}\text{Pu}/^{239}\text{Pu}$, $^{241}\text{Pu}/^{239}\text{Pu}$ and $^{242}\text{Pu}/^{239}\text{Pu}$ in
315 flood sediments are shown on Figure 2, Figure 3 and Figure 4, respectively. These plutonium isotopic
316 ratios provided information regarding the origin and the fate of plutonium in the Niida River catchment.
317 The proportions of plutonium originating from the FDNPP in each sample were then calculated from the
318 isotopic abundances of ^{241}Pu (Figure 5 and Table 3).

319 Although at ultra-trace concentrations (<150 fg/g), the four plutonium isotopes (^{239}Pu , ^{240}Pu , ^{241}Pu and
320 ^{242}Pu) were detected in all the samples, with one exception (soil sample FNS 216). The total plutonium
321 masses measured for this sample remained in the same order of magnitude as those found in the three
322 process blanks (4.5 ± 1.5 fg/g after blank correction). Accordingly, it was concluded that no plutonium
323 was detected in this sample, which was therefore not considered when estimating the proportion of
324 plutonium originating from the FDNPP.

325 In samples where plutonium was detected in significant concentrations, plutonium isotopic ratios
326 generally plotted between the global fallout and FDNPP signatures (Figure 2, 3 and 4), with one
327 exception for the $^{242}\text{Pu}/^{239}\text{Pu}$ atom ratio (FNL661 sample; Figure 4). These results demonstrate that most
328 samples contained a mixture of plutonium from both sources. Following the FDNPP accident, plutonium
329 deposition on soils was likely heterogeneous ([Schneider et al., 2013](#)). When examining plutonium in

330 three aliquots from one single sediment sample, plutonium concentrations remained similar. However,
331 subsamples were characterized by differences in their isotopic ratios (Table 2). Although this sample was
332 mixed and homogenised during the preparation process, plutonium from FDNPP remained
333 heterogeneously distributed within the sample. This suggests that FDNPP-derived plutonium is contained
334 in a limited number of plutonium-containing particles ([Salbu, 2011](#)) randomly distributed in each aliquot
335 ([Kimura et al., 2015](#); [Yamamoto et al., 2014](#)). This heterogeneity could explain the variations (~8%)
336 observed in isotopic ratios when repeating the measurements on the same sample.

337 ***Spatial pattern of initial plutonium soil contamination***

338 In all the soil samples (Figure 1, Table 2), the FDNPP-derived plutonium concentration increased with
339 radiocaesium activities (correlation coefficient of 0.96, *p-value* = 0.03) (Figure S1). The highest FDNPP-
340 originated plutonium concentration (27.5 ± 3.3 fg/g) was found in the sample FNS 141, which contained
341 the highest ^{137}Cs activity (148.3 ± 1.5 kBq/kg). The second most contaminated sample in both plutonium
342 and radiocaesium was sample FNS 135 (with a FDNPP-derived plutonium concentration of 2.3 ± 0.4 fg/g
343 and a ^{137}Cs activity of 47.8 ± 0.5 kBq/kg). Sample FNS 116 contained 0.80 ± 0.33 fg/g of FDNPP-originated
344 plutonium and 17.5 ± 0.2 kBq/kg of ^{137}Cs . Sample FNS 137 contained 0.34 ± 0.31 fg/g of FDNPP-derived
345 plutonium and 8.8 ± 0.1 kBq/kg of ^{137}Cs . Finally, in the sample FNS 216 that was the less impacted by the
346 radiocaesium deposition (1.2 ± 0.1 kBq/kg of ^{137}Cs), no plutonium was measured as already mentioned
347 above, which suggests the absence of FDNPP-derived plutonium input at this location.

348 ***Temporal variations of plutonium in sediment***

349 At the Upstream Zone 1 location, most isotopic ratios measured in sediment ($^{240}\text{Pu}/^{239}\text{Pu}$, $^{241}\text{Pu}/^{239}\text{Pu}$ and
350 $^{242}\text{Pu}/^{239}\text{Pu}$) were higher than the global fallout signature (Table 1) ([Muramatsu et al., 2003](#); [Yang et al.,](#)
351 [2015](#); [Zhang et al., 2010](#)), except for those $^{240}\text{Pu}/^{239}\text{Pu}$ ratios measured in sediment collected in
352 November 2011 and November 2013. In November 2014, all isotopic ratios increased again at Upstream
353 Zone 1 and they were even higher in 2014 than those found in 2011, suggesting a significant transfer of
354 contaminated particles between November 2013 and November 2014 ([Evrard et al., 2013](#); [Lacey et al.,](#)
355 [2016b](#)). This site was the only investigated location potentially impacted by the remediation works
356 ([Evrard et al., 2016](#)). In paddy fields, decontamination consisted of removing and replacing the
357 uppermost 5 cm of topsoil with non-contaminated subsoil. Although decontamination should ultimately
358 remove the most contaminated soil layer, there could be a significant plutonium remobilisation and
359 transport phase from upper catchment areas when a typhoon occurs during the remediation works, as

360 vegetation must be cut in order to prepare these remediation works and soil is left bare and exposed to
361 rainfall and runoff. It should be noted that the $^{242}\text{Pu}/^{239}\text{Pu}$ isotopic ratio found in 2014 was even higher
362 than that associated with the FDNPP fallout ([Kirchner et al., 2012](#); [Nishihara et al., 2012](#); [Schwantes et](#)
363 [al., 2012](#)), likely reflecting uncertainties on the estimation of the FDNPP signature or possible
364 uncorrected interferences for the ^{242}Pu isotope (Table 1) ([Meusburger et al., 2016](#)).

365 At the second sampling location in the upper catchment area (Upstream Zone 2), plutonium masses
366 remained very low (<21 fg/g) and stable with time. Moreover, all isotopic ratios did not change
367 significantly for the three campaigns, with $^{241}\text{Pu}/^{239}\text{Pu}$ and $^{242}\text{Pu}/^{239}\text{Pu}$ remaining systematically higher
368 than the global fallout signature. These results suggest that this area is less exposed to erosion, which is
369 consistent with its location in the restricted access zone where soil cultivation was prohibited and where
370 decontamination works started late in 2016. The material transiting in the river at this location, that may
371 originate from nearby forests, was likely similar during the three campaigns.

372 At Downstream Zone 1, plutonium masses were very low (<20 fg/g) for the three measurements.
373 However, all isotopic ratios decreased with time. The values found in 2011 were higher than the global
374 fallout ratios, reflecting the fact that they contained a significant proportion of FDNPP-derived
375 plutonium. Although the $^{241}\text{Pu}/^{239}\text{Pu}$ ratio in the sample collected in 2013 remained significantly higher
376 than the global fallout signature, this was no longer the case in the sample collected in 2014. These
377 results suggest a rapid and significant flush of contaminated material after typhoons in 2013 and 2014
378 ([Lacey et al., 2016a](#)). Overall, proportions of FDNPP-derived plutonium in these samples decreased by
379 one order of magnitude with time, whereas the concentration of global fallout derived plutonium
380 measured in 2014 was 45% higher than the one measured in 2011. The FDNPP-derived plutonium
381 deposited on the uppermost soil surface layer (~1-2 cm) may have been washed away more rapidly
382 compared to the global fallout plutonium that was likely homogenised in the soil profile (~15 cm) by the
383 prolonged ploughing and puddling of the paddy fields during the last several decades ([Alewell et al.,](#)
384 [2014](#); [Xu et al., 2016](#)).

385 Further downstream, at the Downstream Zone 2 sampling point, all isotopic ratios measured in 2013
386 were lower than those measured in 2011. However, no major difference was observed between the
387 isotopic ratios measured in 2013 and 2014. Moreover, they were significantly higher than the global
388 fallout signature, except for the $^{240}\text{Pu}/^{239}\text{Pu}$ ratio measured in samples collected in November 2013 and
389 2014. Total plutonium concentrations also decreased (-56%) between 2011 and 2014, further
390 demonstrating the progressive flush of contaminated material. During the same period, an 85% decrease

391 in the fraction of FDNPP-derived plutonium was observed, whereas the fraction of global fallout
392 plutonium only decreased by 43%, reflecting again the preferential export of FDNPP-derived plutonium
393 immediately following the accident. This preferential export is likely due to the accumulation of FDNPP-
394 derived plutonium in the upper soil layer, which is the most affected by erosion.

395 ***Comparison of radiocesium and plutonium activities***

396 ^{137}Cs levels measured after the FDNPP accident in soils and river sediment of the investigated region
397 were up to 5 orders of magnitude higher ($10,000\text{--}100,000\text{ Bq kg}^{-1}$) than those prevailing before 2011, i.e.
398 typically 30 Bq kg^{-1} (Fukuyama et al., 2010). Accordingly, all the ^{137}Cs measured in the samples analysed
399 in the current research was considered to originate exclusively from the accident, which was confirmed
400 by the measurements of ^{134}Cs and the calculation of $^{134}\text{Cs}/^{137}\text{Cs}$ activity ratios of 0.9–1.0 (Chartin et al.,
401 2013). Although radiocesium is rapidly bound to clay-sized sediment or material enriched in organic
402 matter following the thermonuclear bomb testing (Motha et al., 2002; Tamura, 1964), these parameters
403 were not found to provide the main factors controlling radionuclide levels measured in soils and
404 sediment collected in Fukushima, as these were mainly driven by the spatial pattern of the initial
405 radioactive fallout and its progressive erosion (Eyrolle-Boyer et al., 2016). Accordingly, in this post-
406 accidental context, no significant relationship was found between ^{137}Cs concentrations and TOC
407 (correlation coefficient of 0.43, p -value = 0.02) or SSA (correlation coefficient of 5×10^{-5}) in samples
408 analysed in the current research. These findings are also consistent with previous results showing that
409 radiocesium contamination was shown to be attached to multiple particle size fractions, including silt-
410 and sand-sized particles (Sakaguchi et al., 2015).

411 $^{239+240}\text{Pu}/^{137}\text{Cs}$ activity ratios in the soil samples (Table 2) remained in a very narrow range ($1.25 - 5.98 \times$
412 10^{-7}) suggesting that plutonium and radiocesium underwent similar deposition processes. In contrast,
413 the corresponding values found in flood sediment deposits varied by several orders of magnitude (from
414 2.39×10^{-8} to 1.19×10^{-5}) reflecting the changes of source contributions to sediment transiting the river
415 throughout time. Other $^{239+240}\text{Pu}/^{137}\text{Cs}$ activity ratios measured in environmental samples collected in the
416 Fukushima region after the FDNPP accident were provided in the literature (Sakaguchi et al., 2014; Zheng
417 et al., 2012b). Zheng et al. (2012b) compared this ratio with that measured after the Chernobyl accident.
418 Yamamoto et al. (2014) estimated that this ratio varied between 2.6×10^{-9} and 4.8×10^{-6} in road dust,
419 litter and soil samples. They observed a positive relationship between this ratio and the distance from
420 the power plant. In the current study, no such relationship was observed, which is likely explained by the
421 fact that all samples were collected relatively far from FDNPP (between 25 - 45 km).

422 However, the spatial variation of this ratio across the catchment may also provide additional information
423 on the processes affecting sediment-bound radionuclide redistribution after the FDNPP accident. The
424 increase in $^{239+240}\text{Pu}/^{137}\text{Cs}$ activity ratios observed at the Upstream Zone 1 sampling location (Table 2)
425 suggests that the remobilisation of plutonium after the completion of remediation works differed from
426 that of radiocesium. In contrast, the $^{239+240}\text{Pu}/^{137}\text{Cs}$ activity ratios at the upstream Zone 2 site did almost
427 not change during the studied period (Table 2), confirming the previous conclusion that this sampling
428 location is less exposed to erosion as it is located in a restricted zone and it is mainly covered with forests
429 which are less sensitive to soil erosion. The same observation can be made for the Downstream Zone 1
430 location, with the absence of significant change (p-value=0.06) in the $^{239+240}\text{Pu}/^{137}\text{Cs}$ activity ratios found
431 at this location between 2011 and 2014 (Table2). This result suggested a simultaneous decrease of
432 plutonium and radiocesium, in the same relative proportions. Finally, at the last sampling location
433 (Downstream 2), the $^{239+240}\text{Pu}/^{137}\text{Cs}$ activity ratios also did not vary significantly (p-value= 0.08),
434 suggesting again a simultaneous decrease of both radionuclide contamination at this site, in the same
435 proportions.

436 **Conclusions and perspectives**

437 In the current research, plutonium concentrations and isotopic ratios were measured in soil and flood
438 sediment collected at various locations in the Niida catchment after the FDNPP accident. Plutonium
439 isotopic ratios associated with the global fallout were shown to be homogeneous and these ratios were
440 therefore used to calculate the respective sources of Pu, in particular the contribution of FDNPP to the
441 total amount of Pu found in these sediment samples. As demonstrated by the soil analyses, the spatial
442 pattern of initial plutonium deposition was similar to that of radiocaesium (Figure 1). In November 2011,
443 isotopic ratios and FDNPP derived-plutonium concentrations were higher in the coastal plain sediment
444 samples than those obtained in upper catchment areas. This suggests that FDNPP plutonium, eroded
445 from the topsoil and transported with sediment particles during floods, was rapidly transported
446 downstream. The analysis of the $^{239+240}\text{Pu}/^{137}\text{Cs}$ activity ratios found in the soil samples confirmed that
447 radiocesium and plutonium underwent similar deposition processes. In general, their redistribution with
448 sediment in the catchment followed the same trends, except at the site affected by remediation works.

449 Although the sampling procedure was rigorously the same during each field campaign and the samples
450 were well-mixed, future research should examine the variability of these sediment deposits along a river
451 reach. Moreover, the number of investigated sites remained limited. The main challenge when analysing
452 the spatial-temporal variations of actinides is related to the very long time (e.g. several weeks) needed to

453 process samples and analyse them for plutonium with MC-ICP-MS. The ongoing development of more
454 rapid measurement techniques may provide solutions in the future for analysing larger sets of samples.
455 For example, some authors recently proposed several improvements in dissolution methods and in
456 chemical separations, which are faster and more efficient ([Bu et al., 2017](#); [Men et al., 2018](#)).

457 Different plutonium isotopic ratios measured in three homogenised aliquots from one sample, suggested
458 the emission of discrete plutonium-bearing particles during the FDNPP accident (Table 4). This result also
459 shows the importance of processing representative samples with a significant quantity of material (e.g.
460 5 g samples in the current research, while others studies compiled in Table S1 processed 1 to 5 g of
461 samples) as plutonium contamination from FDNPP may be in the form of a limited number of discrete
462 plutonium-bearing particles. The characterisation of these particles requires further investigation. The
463 particulate form of FDNPP-derived plutonium must be examined in order to better understand the origin
464 of plutonium from the power plant (mixed-oxide fuel or irradiated UO₂ fuel) and to improve our
465 knowledge of the mechanisms releasing actinides during the FDNPP accident (shape and composition of
466 the emitted particles). These properties should also impact the fate and the residence time of actinides
467 in the environment.

468 Accordingly, to further understand the migration of plutonium in the fallout-impacted region, screening
469 methods should be developed and applied to identify, isolate and characterize plutonium-bearing
470 particles. Elemental and isotopic compositions of these particles should then be measured to determine
471 their source (e.g. formation mechanism in the reactor, source reactor, etc.) and to characterise their fate
472 in the environment (e.g. ability to dissolve, to be remobilized, to be associated with colloids, etc.).

473 **Acknowledgements**

474 This work has been supported by the French National Research Agency (ANR) in the framework of the
475 AMORAD project (ANR-11-RSNR-0002). Hugo Jaegler received a PhD fellowship from the CEA
476 (Commissariat à l'Energie Atomique et aux Energies Alternatives, France). **The authors are grateful to Dr.**
477 **Mercedes Mendez-Millan (LOCEAN laboratory) and Dr. Anthony Foucher (University of Tours) for their**
478 **help to conduct the organic matter and particle size analyses.**

479 **Tables**

480 *Table 1: Estimates of the plutonium isotopic atom ratios in FDNPP at the time of the reactor shutdown*
 481 *and measured isotopic ratios of fallout plutonium in soils of the region representative of global fallout.*
 482 *Uncertainties associated with ratios of global fallout are extended with a confidence level of 95%*
 483 *(coverage factor of 2).*

		$^{240}\text{Pu}/^{239}\text{Pu}$	$^{241}\text{Pu}/^{239}\text{Pu}$	$^{242}\text{Pu}/^{239}\text{Pu}$
FDNPP	Nishihara <i>et al.</i> (2012)			
	Reactor 1	0.344	0.1921	0.0662
	Reactor 2	0.320	0.1922	0.0630
	Reactor 3	0.356	0.1827	0.0620
	Schwantes <i>et al.</i> (2012)	0.447	0.1962	
	Kirchner <i>et al.</i> (2012)	0.395	0.1738	
Mean		0.373 ± 0.044	0.1874 ± 0.0081	0.0637 ± 0.0026
Global Fallout	Kelley <i>et al.</i> (1999)			
	Av. soils NH 30°-71°	0.180 ± 0.014	0.0011 ± 0.0001	0.0039 ± 0.0007
	Sapporo, Japan	0.177 ± 0.002	0.0011 ± 0.0001	0.0038 ± 0.0002
	Tokyo, Japan	0.176 ± 0.002	0.0010 ± 0.0001	0.0035 ± 0.0002
	Zhang <i>et al.</i> (2010)	0.192 ± 0.003	0.0026 ± 0.0003	
	Zhang <i>et al.</i> (2010)	0.192 ± 0.004	0.0029 ± 0.0006	
	Muramatsu <i>et al.</i> (2003)	0.179 ± 0.001		
	Yang <i>et al.</i> (2015)	0.183 ± 0.011		
Mean		0.181 ± 0.005	0.0015 ± 0.0003	0.0037 ± 0.0005

484

485 Table 2: Plutonium concentrations and atom ratios measured in soil and sediment samples collected in the Niida River. Extended uncertainties with a
 486 confidence level of 95% (coverage factor of 2); ²⁴¹Pu/²³⁹Pu values were decay-corrected to 15 March 2011. ²⁴⁰Pu, ²⁴¹Pu and ²⁴²Pu isotopes were not
 487 detected in samples FNS216 and FNL477.

Sample			Location	²⁴⁰ Pu/ ²³⁹ Pu atom ratio	²⁴¹ Pu/ ²³⁹ Pu atom ratio	²⁴² Pu/ ²³⁹ Pu atom ratio	Total plutonium mass concentration (fg/g)	²³⁹⁺²⁴⁰ Pu/ ¹³⁷ Cs (activity ratio)
Soil	FNS116	Apr.2012	-	0.188 ± 0.007	0.0041 ± 0.0009	0.006 ± 0.002	45.7 ± 1.3	1.48×10 ⁻⁷ ± 4.33×10 ⁻⁸
	FNS135	Apr.2012		0.190 ± 0.002	0.0069 ± 0.0004	0.007 ± 0.003	62.9 ± 7.2	1.58×10 ⁻⁷ ± 1.99×10 ⁻⁸
	FNS137	Apr.2012		0.183 ± 0.012	0.0033 ± 0.0014	0.005 ± 0.001	29.7 ± 0.6	1.25×10 ⁻⁷ ± 8.25×10 ⁻⁸
	FNS141	Apr.2012		0.205 ± 0.008	0.0287 ± 0.0018	0.013 ± 0.001	145.2 ± 1.5	5.98×10 ⁻⁷ ± 5.17×10 ⁻⁸
	FNS216	Nov.2012		-	-	-	4.6 ± 1.5	-
Flood Sediment	FNL058 A	Nov.2011	Upstream Zone 1	0.188 ± 0.016	0.0074 ± 0.0042	0.012 ± 0.006	54.5 ± 3.4	1.01×10 ⁻⁷ ± 5.46×10 ⁻⁸
	FNL477	Nov.2013		0.174 ± 0.012	0.0186 ± 0.0036	0.0106 ± 0.0038	44.4 ± 2.31	2.19×10⁻⁶ - 5.15×10⁻⁷
	FNL661	Nov.2014		0.267 ± 0.016	0.0668 ± 0.0100	0.116 ± 0.014	44.5 ± 2.9	1.19×10 ⁻⁵ ± 1.61×10 ⁻⁶
	FNL031 A	Nov.2011	Upstream Zone 2	0.195 ± 0.028	0.0075 ± 0.0019	0.016 ± 0.008	14.6 ± 0.6	2.39×10 ⁻⁸ ± 6.57×10 ⁻⁹
	FNL492	Nov.2013		0.186 ± 0.027	0.0066 ± 0.0015	0.019 ± 0.007	16.2 ± 0.7	3.33×10 ⁻⁸ ± 8.04×10 ⁻⁹
	FNL667	Nov.2014		0.183 ± 0.026	0.0069 ± 0.0023	0.018 ± 0.010	20.3 ± 0.9	4.23×10 ⁻⁸ ± 1.41×10 ⁻⁸
	FNL064	Nov.2011	Downstream Zone 1	0.217 ± 0.023	0.0447 ± 0.0127	0.037 ± 0.012	17.1 ± 2.6	3.33×10 ⁻⁷ ± 8.07×10 ⁻⁸
	FNL468	Nov.2013		0.193 ± 0.028	0.0135 ± 0.0078	0.008 ± 0.005	16.0 ± 0.7	1.01×10 ⁻⁷ ± 4.79×10 ⁻⁸
	FNL685	Nov.2014		0.173 ± 0.022	0.0032 ± 0.0019	0.004 ± 0.002	17.8 ± 0.8	1.09×10 ⁻⁷ ± 1.05×10 ⁻⁷
	FNL043 B	Nov.2011	Downstream Zone 2	0.223 ± 0.007	0.0464 ± 0.0024	0.022 ± 0.002	94.8 ± 15.9	6.52×10 ⁻⁶ ± 9.40×10 ⁻⁷
	FNL465	Nov.2013		0.183 ± 0.007	0.0097 ± 0.0018	0.010 ± 0.002	48.1 ± 8.6	4.19×10 ⁻⁷ ± 9.16×10 ⁻⁸
	FNL688	Nov.2014		0.174 ± 0.008	0.0158 ± 0.0041	0.009 ± 0.003	42.0 ± 7.7	6.23×10 ⁻⁶ ± 1.60×10 ⁻⁶

489 Table 3: Relative contributions and concentrations of FDNPP and global fallout plutonium in the analysed
 490 samples, modelled with ²⁴¹Pu measurements. Uncertainties are extended with a confidence level of 95%
 491 (coverage factor of 2).

Sample	Date of sampling	Location	Proportion of Plutonium from FDNPP	Plutonium concentration from FDNPP in the samples (fg/g)	Plutonium concentration from global fallout in the samples (fg/g)	
Soil	FNS116	Apr.2012	1.9 % ± 0.7 %	0.9 ± 0.3	44.8 ± 1.3	
	FNS135	Apr.2012	3.9 % ± 0.5 %	2.4 ± 0.4	60.5 ± 7.3	
	FNS137	Apr.2012	1.3 % ± 1.1 %	0.4 ± 0.3	29.3 ± 0.6	
	FNS141	Apr.2012	19.1 % ± 2.3 %	27.7 ± 3.3	117.5 ± 3.7	
	FNS216	Nov.2012	-	-	-	
Flood Sediment	FNLO58A	Nov. 2011	Upstream Zone 1	4.3 % ± 3.1 %	2.3 ± 1.7	52.1 ± 3.8
	FNL477	Nov. 2013	Upstream Zone 1	12.4 % ± 2.9 %	5.5 ± 1.3	38.9 ± 2.7
	FNL661	Nov. 2014	Upstream Zone 1	39.3 % ± 7.0 %	17.5 ± 3.3	27.0 ± 4.4
	FNLO31A	Nov. 2011	Upstream Zone 2	3.7 % ± 1.4 %	0.5 ± 0.2	14.0 ± 0.7
	FNL492	Nov. 2013	Upstream Zone 2	3.6 % ± 1.2 %	0.6 ± 0.2	15.6 ± 0.7
	FNL667	Nov. 2014	Upstream Zone 2	3.9 % ± 1.7 %	0.8 ± 0.4	19.5 ± 0.9
	FNL064	Nov. 2011	Downstream Zone 1	29.0 % ± 8.8 %	5.0 ± 1.7	12.1 ± 3.1
	FNL468	Nov. 2013	Downstream Zone 1	8.6 % ± 5.6 %	1.4 ± 0.9	14.6 ± 1.2
	FNL685	Nov. 2014	Downstream Zone 1	1.2 % ± 1.4 %	0.2 ± 0.3	17.6 ± 0.8
	FNLO43B	Nov. 2011	Downstream Zone 2	30.3 % ± 3.4 %	28.8 ± 5.8	65.9 ± 17.0
	FNL465	Nov. 2013	Downstream Zone 2	5.9 % ± 1.4 %	2.9 ± 0.9	45.2 ± 8.6
	FNL688	Nov. 2014	Downstream Zone 2	10.4 % ± 3.1 %	4.4 ± 1.5	37.6 ± 7.8

492

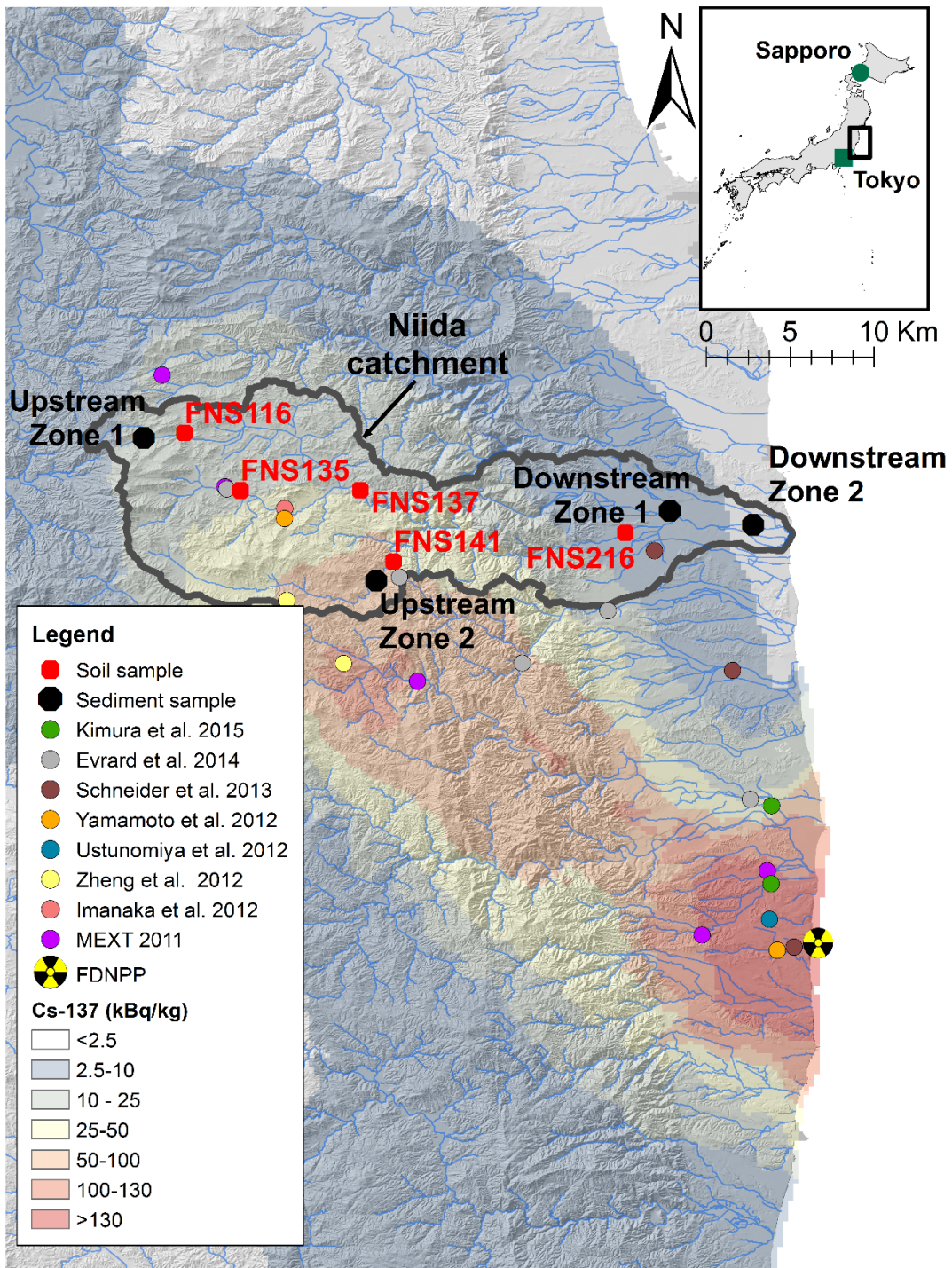
493 Table 4: Plutonium isotopic ratios and concentrations for a sample divided into three aliquots.
 494 Uncertainties are extended with a confidence level of 95% (coverage factor of 2)

Sample	Date of sampling	Location	²⁴⁰ Pu / ²³⁹ Pu atom ratio	²⁴¹ Pu / ²³⁹ Pu atom ratio	²⁴² Pu / ²³⁹ Pu atom ratio	Total plutonium mass concentration (fg/g)
FNL492 - 1	Nov.2013	Upstream Zone 2	0.188 ± 0.027	0.0145 ± 0.0029	0.048 ± 0.012	14.82 ± 0.62
FNL492 - 2	Nov.2013		0.184 ± 0.026	0.0069 ± 0.0018	0.018 ± 0.008	15.81 ± 0.68
FNL492 - 3	Nov.2013		0.177 ± 0.026	0.0081 ± 0.0022	0.010 ± 0.009	17.92 ± 0.78

495

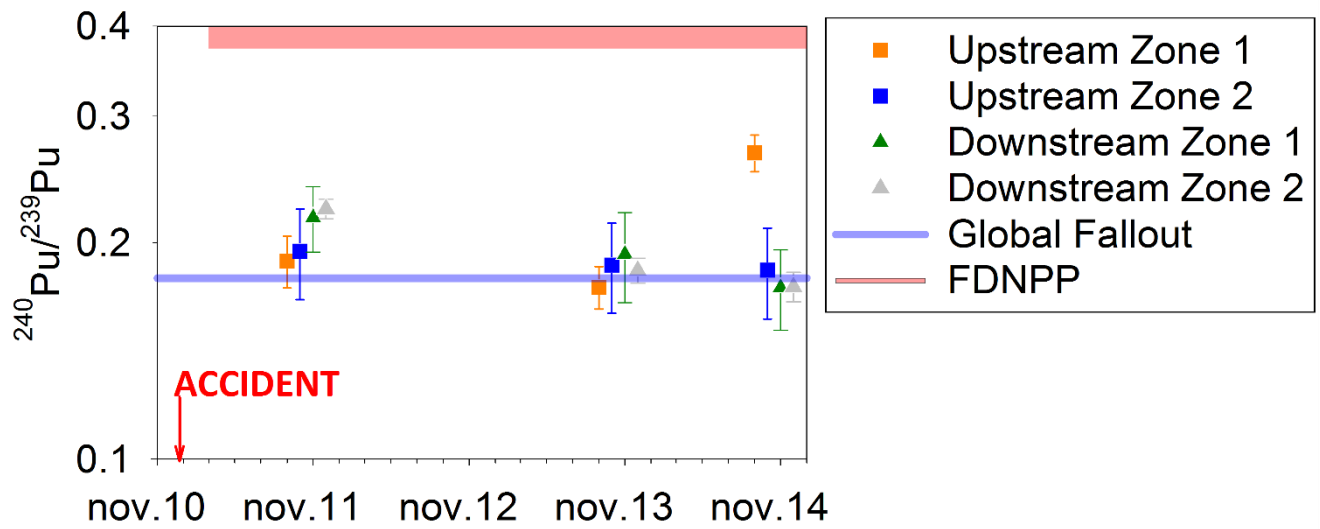
496

497



499 Figure 1: Location of soil and sediment samples containing FDNPP-derived plutonium from literature and
 500 location of samples analysed in this current research in the Niida catchment delineated in black. The
 501 main radiocaesium contamination plume is also located in the background map derived from Chartin et
 502 al. (2013).

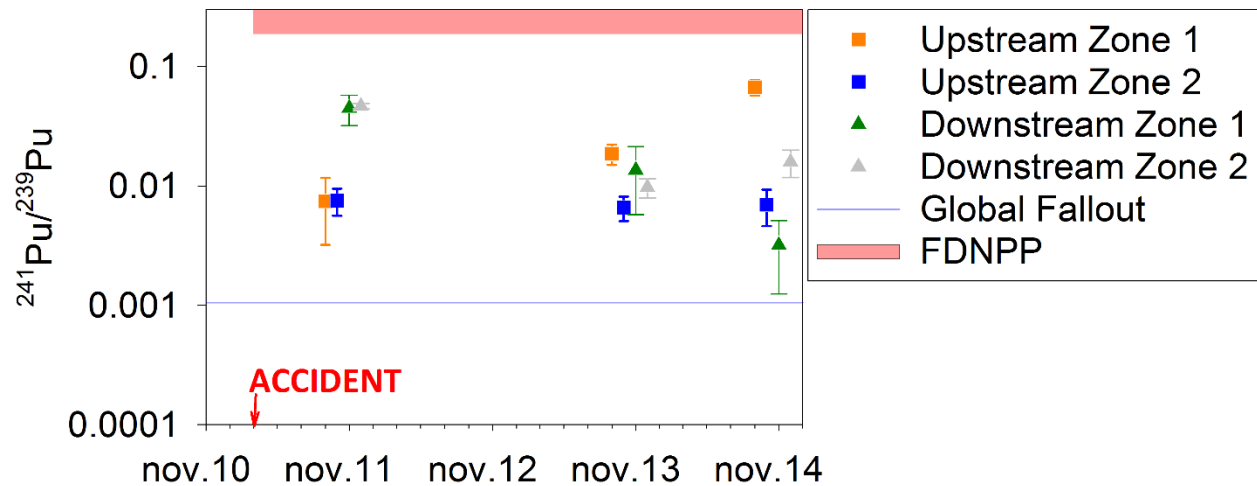
503



504

505 Figure 2: $^{240}\text{Pu}/^{239}\text{Pu}$ atomic ratios measured in this study. The blue line corresponds to the mean global
 506 fallout value ([Kelley et al., 1999](#); [Muramatsu et al., 2003](#); [Yang et al., 2015](#); [Zhang et al., 2010](#)), the red
 507 line corresponds to estimations of the FDNPP signature ([Kirchner et al., 2012](#); [Nishihara et al., 2012](#);
 508 [Schwantes et al., 2012](#)). Uncertainties are extended with a confidence level of 95% (coverage factor of
 509 2).

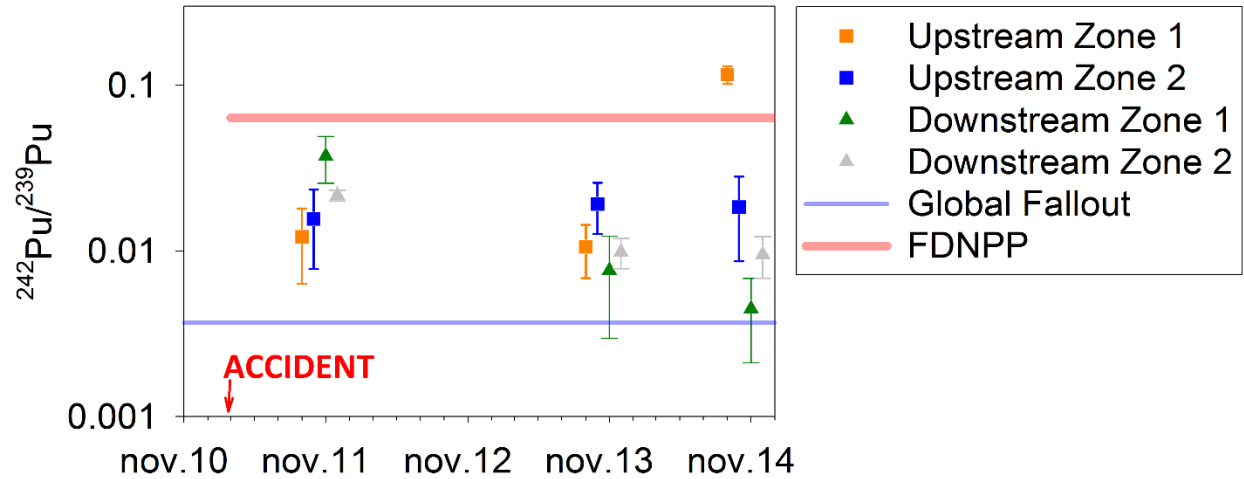
510



511

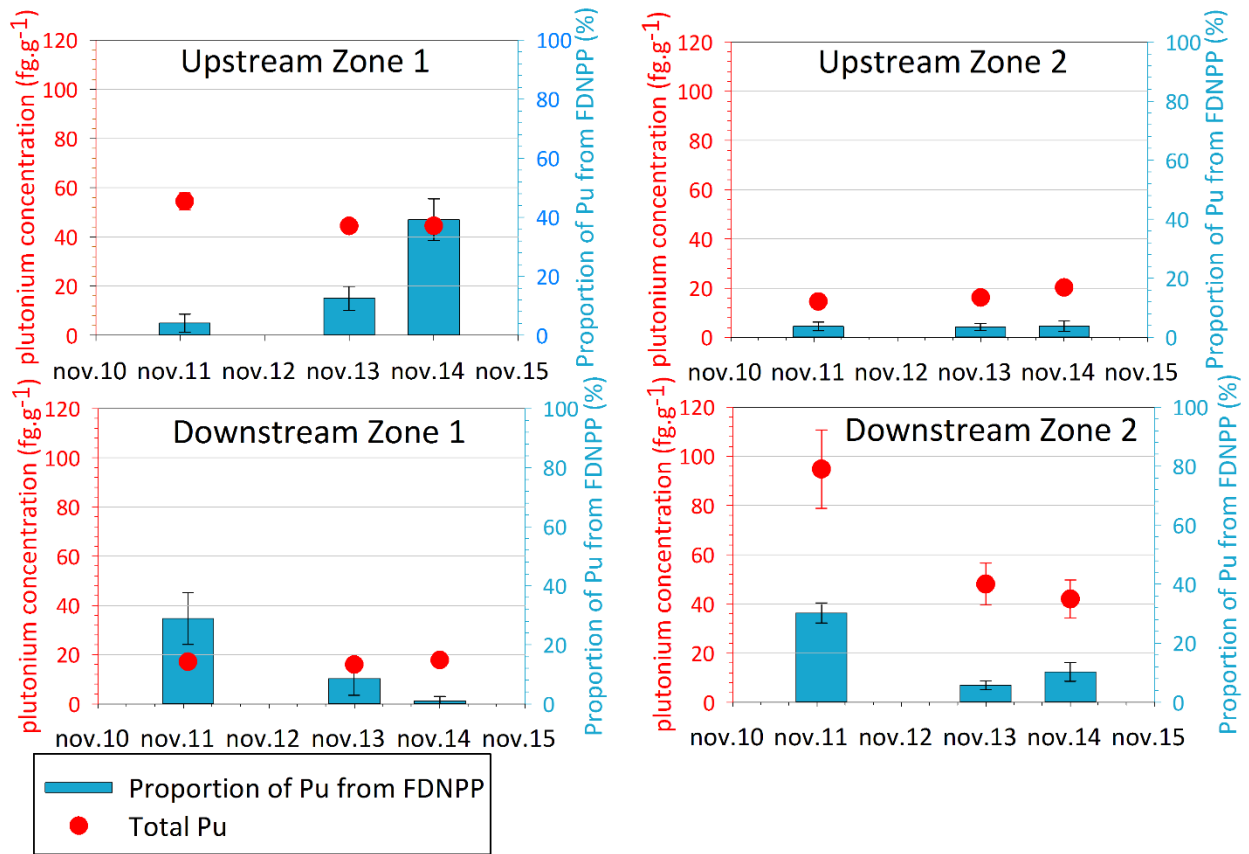
512 Figure 3: $^{241}\text{Pu}/^{239}\text{Pu}$ atomic ratios measured in this study. The blue line corresponds to the mean global
 513 fallout value ([Kelley et al., 1999](#); [Zhang et al., 2010](#)), the red line corresponds to estimations of the
 514 FDNPP signature ([Kirchner et al., 2012](#); [Nishihara et al., 2012](#); [Schwantes et al., 2012](#)). Uncertainties are
 515 extended with a confidence level of 95% (coverage factor of 2). Numbers of ^{241}Pu atoms were decay-
 516 corrected to 15 March 2011.

517



518 Figure 4: $^{242}\text{Pu}/^{239}\text{Pu}$ atomic ratios measured in this study. The blue line corresponds to the mean global
 519 fallout value (Kelley et al., 1999), the red line corresponds to estimations of the FDNPP signature
 520 (Kirchner et al., 2012; Nishihara et al., 2012; Schwantes et al., 2012). Uncertainties are extended with a
 521 confidence level of 95% (coverage factor of 2).

522



523

524 Figure 5: Total plutonium concentrations in all samples (red dots) and contributions of FDNPP-originating
 525 plutonium (blue histograms) deduced from the ²⁴¹Pu abundances in each sample. Uncertainties are
 526 extended with a confidence level of 95% (coverage factor of 2).

527 **Supplementary Information:**

528 Table S1: Plutonium isotopic ratios measured in environmental samples collected in Japan after the FDNPP accident (PPG refers to the Pacific
529 Proving Ground).

Measurement technique	Source	Sample types	Sampling date	Direction (and distance from FDNPP in km)	²⁴⁰ Pu/ ²³⁹ Pu atom ratio	²⁴¹ Pu/ ²³⁹ Pu atom ratio	²⁴¹ Pu/ ²³⁹⁺²⁴⁰ Pu activity ratio	²³⁸ Pu/ ²³⁹⁺²⁴⁰ Pu activity ratio
ICP-MS	Zheng <i>et al.</i> (2012b)	Litter and surface soil (n=7)	April – Aug., 2011	NW (26–32)	0.323-0.330	0.128-0.135	107.8	-
		Soil (n=12)		S (20)	0.303	0.103	-	-
				SW (130–230)	0.171 - 0.303	-	-	-
	Schneider <i>et al.</i> (2013)	Soil (n=13) and plant (n=7)	Oct. – Dec 2011	NW and SW (1 – 244)	0.381 - 0.64	-	-	-
	Evrard <i>et al.</i> (2014b)	River sediment (n=6)	Nov. 2011 – May 2013	NW (10–70)	0.150 - 0.281	0.0019-0.100	2.0–82.3	-
	Zheng <i>et al.</i> (2012a)	Marine surface sediments (n=9)	July – Aug. 2011	NE (200)	0.188, 0.189	0.0034	-	-
				E (30–200)	0.22 - 0.26 (PPG)	-	-	-
	Sakaguchi <i>et al.</i> (2012)	River water (n=1)	June – Aug. 2011	NW (70)	0.308	-	-	-
Seawater (n=2)		E (30)		0.181 - 0.218 (PPG)	-	-	-	
Alpha-spectrometry	MEXT(2011)	Surface soils (n=5)	June – July 2011	NW (5–100)	-	-	-	0.33 – 2.2
	Yamamoto <i>et al.</i> (2014)	Soil (n=8)	2011 – 2012	NW (20–30)	-	-	-	0.088-1.324
	Imanaka <i>et al.</i> (2012)	Soil (n=3)	28 – 29 March 2011	NW (30)	-	-	-	0.110-1.324
	Utsunomiya <i>et al.</i> (2012)	Sediment (n=5)	No information	NW (3)	-	-	-	0.319-2.60
	Kimura <i>et al.</i> (2015)	Soil (n=6)	No information	NW (4)	-	-	-	0.22-1.54

531 Table S2: Location of the investigated samples.

Sample		Date of sampling	Location	GPS coordinates	
				Y	X
Soil	FNS116	Apr.2012	-	37.693042	140.698035
	FNS135	Apr.2012		37.662240	140.728147
	FNS137	Apr.2012		37.662406	140.791832
	FNS141	Apr.2012		37.624151	140.810154
	FNS216	Nov.2012		37.63945	140.933293
Flood Sediment	FNL058A	Nov.2011	Upstream Zone 1	37.690509	140.676251
	FNL477	Nov.2013			
	FNL661	Nov.2014			
	FNL031A	Nov.2011	Upstream Zone 2	37.61385	140.800832
	FNL492	Nov.2013			
	FNL667	Nov.2014			
	FNL064	Nov.2011	Downstream Zone 1	37.651338	140.958329
	FNL468	Nov.2013			
	FNL685	Nov.2014			
	FNL043B	Nov.2011	Downstream Zone 2	37.643776	141.00301
	FNL465	Nov.2013			
FNL688	Nov.2014				

532

533 **Detector configurations**

534 Gain corrections were determined with minor U isotopes in calibration standard. Accordingly,
 535 measurements were performed in the same level of ion beams signals as those of Pu isotopes in the
 536 samples. This avoided the potential problems of non-linearity of the ion counters. Moreover, for
 537 determining gain factors, the U concentration level was chosen in order to measure the $^{235}\text{U}/^{238}\text{U}$ ratio in
 538 Faraday cups. An “internal” mass bias factor could then be determined. This internal mass bias allowed
 539 to correct for mass bias without using those corrections determined with standard bracketing. The ion
 540 counter IC1, IC3 and IC4 gain factors were respectively determined with $^{236}\text{U}/^{238}\text{U}$, $^{234}\text{U}/^{238}\text{U}$ and $^{233}\text{U}/^{238}\text{U}$
 541 ratios in a mixed solution of uranium standards IRMM186 and IRMM057. The IC2 gain factor was
 542 determined with ^{235}U measured once in IC2 and once in L5 cup. Finally, the IC5 gain factor was calculated
 543 with a third measurement of $^{235}\text{U}/^{238}\text{U}$ conducted on the mixed solution of IRMM 186 and IRMM 057.

544 Table S3: Detector configurations for plutonium samples and uranium standard measurements on MC
 545 ICP-MS. Isotopes measured on ion counting detectors are presented in bold. a: for measurement of peak
 546 tail at m+1 + uranium hydride ratio, b: for measurement of peak tail at m+2.

Cup		IC4	IC3	IC2/L5	IC1	L4	IC5	L2	H1	H3
Pu samples		^{239}Pu	^{240}Pu	^{241}Pu	^{242}Pu		^{244}Pu			
IRMM 186	Mass bias								^{235}U	^{238}U
	Hydrides, tail	$^{239}\text{Pu}^a$	$^{240}\text{Pu}^b$							
IRMM 186 + IRMM 057	Gain Factor IC1, IC3, IC4	^{233}U	^{234}U	^{235}U	^{236}U	^{238}U				
	Gain Factor IC2	^{233}U	^{234}U	^{235}U	^{236}U	^{238}U				
	Gain Factor IC5						^{235}U	^{238}U		

547

548 Table S4: Comparison of plutonium measurements and certified values in IAEA reference materials.
 549 Uncertainties are extended with a confidence level of 95% (coverage factor of 2).

Material	Measured $^{239+240}\text{Pu}$	Certified $^{239+240}\text{Pu}$
IAEA – 385	2.83 ± 0.19	2.89 – 3.00
IAEA – 447	3.70 ± 1.77	4.90 – 5.70

551

552

553

554 Table S5: Calculated plutonium masses in process blanks and in soluble and insoluble fractions after
 555 blank corrections. Uncertainties are extended with a confidence level of 95% (coverage factor of 2).

	Sample masses (g)	Plutonium masses in the soluble fraction (fg)		Plutonium masses in the insoluble fraction (fg)	
Process Blank 1	-	1.2	± 0.4	0.3	± 0.3
Process Blank 2	-	0.3	± 1.2	0.6	± 0.3
Process Blank 3	-	1.9	± 0.5	0.5	± 0.3
Average blank		1.1	± 0.4	0.5	± 0.4
FNL 043B	3.5	324	± 56	14.9	± 2.3
FNL 465	3.9	184	± 33	7.0	± 1.6
FNL 688	4.7	196	± 36	4.9	± 1.0

556

557 Table S6 : Activities in ²³⁹⁺²⁴⁰Pu and ¹³⁷Cs in soil and sediment samples collected in the Niida River
 558 catchment. Extended uncertainties with a confidence level of 95% (coverage factor of 2).

Sample		Date of sampling	Location	²³⁹⁺²⁴⁰ Pu (Bq/kg)	¹³⁷ Cs (kBq/kg)
Soil	FNS116	Apr.2012	-	0.003 ± 0.001	17.5 ± 0.2
	FNS135	Apr.012		0.008 ± 0.001	47.8 ± 0.5
	FNS137	Apr.2012		0.001 ± 0.001	8.8 ± 0.1
	FNS141	Apr.2012		0.47 ± 0.008	148.3 ± 1.5
	FNS216	Nov.2012		-	1.2 ± 0.1
Flood Sediment	FNL058A	Nov.2011	Upstream Zone 1	0.007 ± 0.004	71.0 ± 0.5
	FNL477	Nov.2013		-	8.0 - 0.2
	FNL661	Nov.2014		0.055 ± 0.007	4.6 ± 0.1
	FNL031A	Nov.2011	Upstream Zone 2	0.002 ± 0.000	73.6 ± 0.5
	FNL492	Nov.2013		0.002 ± 0.000	54.0 ± 0.5
	FNL667	Nov.2014		0.002 ± 0.001	57.2 ± 0.5
	FNL064	Nov.2011	Downstream Zone 1	0.016 ± 0.004	47.1 ± 0.3
	FNL468	Nov.2013		0.004 ± 0.002	43.5 ± 0.4
	FNL685	Nov.2014		0.001 ± 0.001	5.6 ± 0.1
	FNL043B	Nov.2011	Downstream Zone 2	0.093 ± 0.013	14.2 ± 0.3
	FNL465	Nov.2013		0.009 ± 0.002	21.1 ± 0.2
FNL688	Nov.2014	0.014 ± 0.003		2.2 ± 0.1	

559

560

561

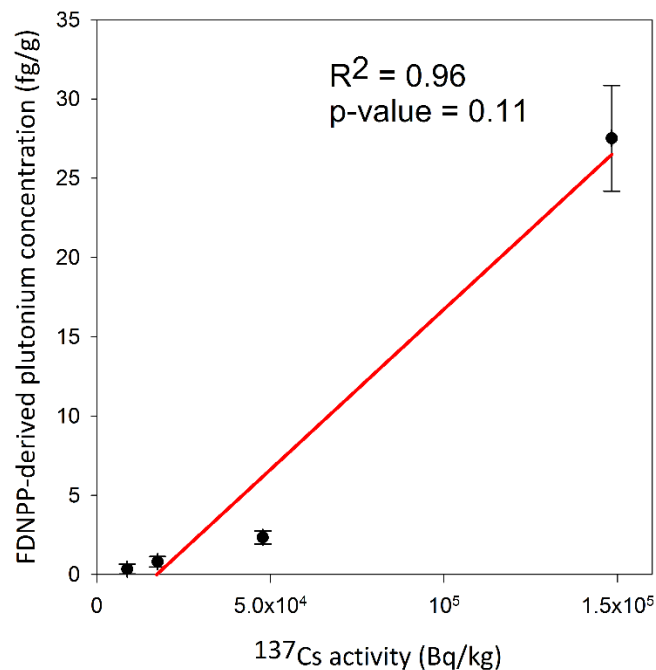
562

563

564 Table S7 : Particulate matter properties and particle size parameters measured in soil and river sediment
 565 samples collected in the Niida River catchment. D50 is the median diameter of the grains. SSA is the
 566 Specific Surface Area. Extended uncertainties with a confidence level of 95% (coverage factor of 2). n.a.:
 567 not available.

	Sample	Date of sampling	Location	Total Organic Carbon (%)	$\delta^{13}\text{C}$ (‰)	D50 (μm)	SSA (m^2/kg)
Soil	FNS116	Apr.2012	-	1.97 ± 0.05	-25.84	79.90	207.93
	FNS135	Apr.012		6.11 ± 0.11	-25.73	189.33	136.33
	FNS137	Apr.2012		3.29 ± 0.08	-26.23	96.70	207.93
	FNS141	Apr.2012		7.75 ± 0.14	-27.77	64.00	349.47
	FNS216	Nov.2012		2.11 ± 0.06	-26.47	137.50	214.35
Flood Sediment	FNL058A	Nov.2011	Upstream Zone 1	n.a.	n.a.	n.a.	n.a.
	FNL477	Nov.2013		5.00 ± 0.10	-27.10	46.23	325.1
	FNL661	Nov.2014		3.96 ± 0.10	-27.09	75.13	198.97
	FNL031A	Nov.2011	Upstream Zone 2	3.47 ± 0.08	-26.83	235	48.91
	FNL492	Nov.2013		4.04 ± 0.09	-27.51	175.00	80.72
	FNL667	Nov.2014		4.80 ± 0.09	-27.01	118.00	92.29
	FNL064	Nov.2011	Downstream Zone 1	4.57 ± 0.11	-28.37	n.a.	n.a.
	FNL468	Nov.2013		2.67 ± 0.10	-28.20	208.67	93.44
	FNL685	Nov.2014		8.47 ± 0.07	-27.31	n.a.	n.a.
	FNL043B	Nov.2011	Downstream Zone 2	6.73 ± 0.14	-27.80	n.a.	n.a.
	FNL465	Nov.2013		2.38 ± 0.12	-28.06	n.a.	n.a.
	FNL688	Nov.2014		3.47 ± 0.06	-24.37	130.00	238.53

568 Figure S1: Correlation between FDNPP-derived plutonium concentration and ^{137}Cs activities in soil
 569 samples. Uncertainties are extended with a confidence level of 95% (coverage factor of 2).



570

571 **References**

572

573

574 Alewell, C., Meusburger, K., Juretzko, G., Mabit, L., Ketterer, M.E. (2014) Suitability of $^{239+240}\text{Pu}$ and
575 ^{137}Cs as tracers for soil erosion assessment in mountain grasslands. *Chemosphere* 103, 274-280.

576 Bailly du Bois, P., Laguionie, P., Boust, D., Korsakissok, I., Didier, D., Fievet, B. (2012) Estimation of marine
577 source-term following Fukushima Dai-ichi accident. *Journal of Environmental Radioactivity* 114, 2-9.

578 Bu, W., Fukuda, M., Zheng, J., Aono, T., Ishimaru, T., Kanda, J., Yang, G., Tagami, K., Uchida, S., Guo, Q.,
579 Yamada, M. (2014) Release of Pu isotopes from the Fukushima Daiichi Nuclear Power Plant accident to
580 the marine environment was negligible. *Environmental Science & Technology* 48, 9070-9078.

581 Bu, W., Zheng, J., Guo, Q., Xiao, D., Aono, T. (2017) Determination of Pu isotopes in sediment and soil
582 samples by SF-ICP-MS: an improved anion-exchange procedure for Pu separation. *Journal of*
583 *Radioanalytical and Nuclear Chemistry*.

584 Chartin, C., Evrard, O., Onda, Y., Patin, J., Lefèvre, I., Otlé, C., Ayrault, S., Lepage, H., Bonté, P. (2013)
585 Tracking the early dispersion of contaminated sediment along rivers draining the Fukushima radioactive
586 pollution plume. *Anthropocene* 1, 23-34.

587 Chiappini, R., Pointurier, F., Millies-Lacroix, J.C., Lepetit, G., Hemet, P. (1999) $^{240}\text{Pu}/^{239}\text{Pu}$ isotopic ratios
588 and $^{239+240}\text{Pu}$ total measurements in surface and deep waters around Mururoa and Fangataufa atolls
589 compared with Rangiroa atoll (French Polynesia). *Science of The Total Environment* 237-238, 269-276.

590 Estournel, C., Bosc, E., Bocquet, M., Ulses, C., Marsaleix, P., Winiarek, V., Osvath, I., Nguyen, C., Duhaut,
591 T., Lyard, F., Michaud, H., Auclair, F. (2012) Assessment of the amount of cesium-137 released into the
592 Pacific Ocean after the Fukushima accident and analysis of its dispersion in Japanese coastal waters.
593 *Journal of Geophysical Research: Oceans* 117, n/a-n/a.

594 Evrard, O., Chartin, C., Onda, Y., Lepage, H., Cerdan, O., Lefèvre, I., Ayrault, S. (2014a) Renewed soil
595 erosion and remobilisation of radioactive sediment in Fukushima coastal rivers after the 2013 typhoons.
596 *Scientific Reports* 4.

597 Evrard, O., Chartin, C., Onda, Y., Patin, J., Lepage, H., Lefevre, I., Ayrault, S., Otlé, C., Bonté, P. (2013)
598 Evolution of radioactive dose rates in fresh sediment deposits along coastal rivers draining Fukushima
599 contamination plume. *Scientific Reports* 3, 3079.

600 Evrard, O., Laceby, J.P., Lepage, H., Onda, Y., Cerdan, O., Ayrault, S. (2015) Radiocesium transfer from
601 hillslopes to the Pacific Ocean after the Fukushima Nuclear Power Plant accident: A review. *Journal of*
602 *Environmental Radioactivity* 148, 92-110.

603 Evrard, O., Laceby, J.P., Onda, Y., Wakiyama, Y., Jaegler, H., Lefèvre, I. (2016) Quantifying the dilution of
604 the radiocesium contamination in Fukushima coastal river sediment (2011-2015). *Scientific Reports* 6,
605 34828.

606 Evrard, O., Pointurier, F., Onda, Y., Chartin, C., Hubert, A., Lepage, H., Pottin, A.C., Lefevre, I., Bonte, P.,
607 Laceby, J.P., Ayrault, S. (2014b) Novel insights into Fukushima nuclear accident from isotopic evidence of
608 plutonium spread along coastal rivers. *Environmental Science & Technology* 48, 9334-9340.

609 Eyrolle-Boyer, F., Boyer, P., Garcia-Sanchez, L., Métivier, J.-M., Onda, Y., De Vismes, A., Cagnat, X., Boulet,
610 B., Cossonnet, C. (2016) Behaviour of radiocaesium in coastal rivers of the Fukushima Prefecture (Japan)
611 during conditions of low flow and low turbidity – Insight on the possible role of small particles and
612 detrital organic compounds. *Journal of Environmental Radioactivity* 151, 328-340.

613 Fukuyama, T., Onda, Y., Gomi, T., Yamamoto, K., Kondo, N., Miyata, S., Kosugi, K.i., Mizugaki, S.,
614 Tsubonuma, N. (2010) Quantifying the impact of forest management practice on the runoff of the
615 surface-derived suspended sediment using fallout radionuclides. *Hydrological Processes* 24, 596-607.

616 Hardy, E.P., Krey, P.W., Volchok, H.L. (1973) Global Inventory and Distribution of Fallout Plutonium.
617 *Nature* 241, 444-445.

618 Harley, J.H. (1979) Plutonium in the environment - A review. *Japan Radiation Research* 21.

619 Imanaka, T., Endo, S., Sugai, M., Ozawa, S., Shizuma, K., Yamamoto, M. (2012) Early radiation survey of
620 litate village, which was heavily contaminated by the Fukushima Daiichi accident, conducted on 28 and
621 29 March 2011. *Health Physics Society* 102, 680-686.

622 Kawamura, H., Kobayashi, T., Furuno, A., In, T., Ishikawa, Y., Nakayama, T., Shima, S., Awaji, T. (2011)
623 Preliminary Numerical Experiments on Oceanic Dispersion of I-131 and Cs-137 Discharged into the Ocean
624 because of the Fukushima Daiichi Nuclear Power Plant Disaster. *Journal of Nuclear Science and*
625 *Technology* 48, 1349-1356.

626 Kelley, J.M., Bond, L.A., Beasley, T.M. (1999) Global distribution of Pu isotopes and ²³⁷Np. *Science of The*
627 *Total Environment* 237–238, 483-500.

628 Kersting, A.B. (2013) Plutonium transport in the environment. *Inorg Chem* 52, 3533-3546.

629 Ketterer, M.E., Hafer, K.M., Link, C.L., Kolwaite, D., Wilson, J., Mietelski, J.W. (2004) Resolving global
630 versus local/regional Pu sources in the environment using sector ICP-MS Presented at the 2003 European
631 Winter Conference on Plasma Spectrochemistry, Garmisch-Partenkirchen, Germany, January 12-17,
632 2003. *Journal of Analytical Atomic Spectrometry* 19, 241.

633 Kimura, H., Uesugi, M., Muneda, A., Watanabe, R., Yokoyama, A., Nakanishi, T. (2015) The situation of Ag
634 and Pu radioisotopes in soil released from Fukushima Daiichi nuclear power plants. *Journal of*
635 *Radioanalytical and Nuclear Chemistry* 303, 1469-1471.

636 Kirchner, G., Bossew, P., De Cort, M. (2012) Radioactivity from Fukushima Dai-ichi in air over Europe; part
637 2: what can it tell us about the accident? *Journal of Environmental Radioactivity* 114, 35-40.

638 Laceby, J.P., Chartin, C., Evrard, O., Onda, Y., Garcia-Sanchez, L., Cerdan, O. (2016a) Rainfall erosivity in
639 catchments contaminated with fallout from the Fukushima Daiichi nuclear power plant accident.
640 *Hydrology and Earth System Sciences* 20, 2467-2482.

641 Laceby, J.P., Huon, S., Onda, Y., Vaury, V., Evrard, O. (2016b) Do forests represent a long-term source of
642 contaminated particulate matter in the Fukushima Prefecture? *Journal of Environmental Management*.

643 Lal, R., Fifield, L.K., Tims, S.G., Wasson, R.J., Howe, D. (2015) Using ²³⁹Pu as a tracer for fine sediment
644 sources in the Daly River, Northern Australia. *EPJ Web of Conferences* 91, 00006.

645 Lepage, H., Laceby, J.P., Bonté, P., Joron, J.-L., Onda, Y., Lefèvre, I., Ayrault, S., Evrard, O. (2016)
646 Investigating the source of radiocesium contaminated sediment in two Fukushima coastal catchments
647 with sediment tracing techniques. *Anthropocene*.

648 Men, W., Zheng, J., Wang, H., Ni, Y., Aono, T., Maxwell, S.L., Tagami, K., Uchida, S., Yamada, M. (2018)
649 Establishing rapid analysis of Pu isotopes in seawater to study the impact of Fukushima nuclear accident
650 in the Northwest Pacific. *Scientific Reports* 8, 1892.

651 Meusburger, K., Mabit, L., Ketterer, M., Park, J.-H., Sandor, T., Porto, P., Alewell, C. (2016) A multi-
652 radionuclide approach to evaluate the suitability of ²³⁹ + ²⁴⁰Pu as soil erosion tracer. *Science of The*
653 *Total Environment* 566–567, 1489-1499.

654 MEXT - Ministry of Education, C., Sports, Sciences and Technology (2011) Results of the Nuclide Analysis
655 of Plutonium and Strontium by MEXT.

656 Ministry of Land Infrastructure and Transport (2006) Rivers in Japan.

657 Motha, J.A., Wallbrink, P.J., Hairsine, P.B., Grayson, R.B. (2002) Tracer properties of eroded sediment and
658 source material. *Hydrological Processes* 16, 1983-2000.

659 Muramatsu, Y., Yoshida, S., Tanaka, A. (2003) Determination of Pu concentration and its isotope ratio in
660 Japanese soils by HR-ICP-MS. *Journal of Radioanalytical and Nuclear Chemistry* 255, 477-480.

661 Nishihara, K., Iwamoto, H., Suyama, K. (2012) Estimation of fuel compositions in Fukushima-Daiichi
662 nuclear power plant. JAEA-Data/Code 2012, <http://jolissrch-inter.tokai-sc.jaea.go.jp/pdfdata/JAEA-Data-Code-2012-018.pdf>
663 (2012)(Date of access: 29/02/2016).

664 Olley, J., Brooks, A., Spencer, J., Pietsch, T., Borombovits, D. (2013) Subsoil erosion dominates the supply
665 of fine sediment to rivers draining into Princess Charlotte Bay, Australia. *Journal of Environmental*
666 *Radioactivity* 124, 121-129.

667 Pointurier, F., Hubert, A., Faure, A.L., Hemet, P., Pottin, A.C. (2011) Polyatomic interferences in
668 plutonium determination in the femtogram range by double-focusing sector-field ICP-MS. *Journal of*
669 *Analytical Atomic Spectrometry* 26, 1474-1480.

670 Rosner, G., Hötzl, H., Winkler, R. (1992) Determination of ²⁴¹Pu by low level B-proportional counting.
671 Application to Chernobyl fallout samples and comparison with the ²⁴¹Am Build-Up Method. *Journal of*
672 *Radioanalytical and Nuclear Chemistry* 163, 225-233.

673 Sakaguchi, A., Kadokura, A., Steier, P., Tanaka, K., Takahashi, Y., Chiga, H., Matsushima, A., Nakashima, S.,
674 Onda, Y. (2012) Isotopic determination of U, Pu and Cs in environmental waters following the Fukushima
675 Daiichi Nuclear Power Plant accident. *Geochemical Journal* 46, 355-360.

676 Sakaguchi, A., Steier, P., Takahashi, Y., Yamamoto, M. (2014) Isotopic Compositions of ²³⁶U and Pu
677 Isotopes in “Black Substances” Collected from Roadsides in Fukushima Prefecture: Fallout from the
678 Fukushima Dai-ichi Nuclear Power Plant Accident. *Environmental Science & Technology* 48, 3691-3697.

679 Sakaguchi, A., Tanaka, K., Iwatani, H., Chiga, H., Fan, Q., Onda, Y., Takahashi, Y. (2015) Size distribution
680 studies of ¹³⁷Cs in river water in the Abukuma Riverine system following the Fukushima Dai-ichi Nuclear
681 Power Plant accident. *Journal of Environmental Radioactivity* 139, 379-389.

682 Salbu, B. (2011) Radionuclides released to the environment following nuclear events. *Integrated*
683 *Environmental Assessment and Management* 7, 362-364.

684 Schneider, S., Walther, C., Bister, S., Schauer, V., Christl, M., Synal, H.-A., Shozugawa, K., Steinhauser, G.
685 (2013) Plutonium release from Fukushima Daiichi fosters the need for more detailed investigations.
686 *Scientific Reports* 3.

687 Schwantes, J.M., Orton, C.R., Clark, R.A. (2012) Analysis of a Nuclear Accident: Fission and Activation
688 Product Releases from the Fukushima Daiichi Nuclear Facility as Remote Indicators of Source
689 Identification, Extent of Release, and State of Damaged Spent Nuclear Fuel. *Environmental Science &*
690 *Technology* 46, 8621-8627.

691 Steinhauser, G. (2014) Fukushima's forgotten radionuclides: a review of the understudied radioactive
692 emissions. *Environmental Science & Technology* 48, 4649-4663.

693 Tamura, T. (1964) Consequences of activity release: selective sorption reactions of cesium with soil
694 minerals. *Nuclear Safety* 5, 262 - 268.

695 TEPCO (2012) Result of estimation of the released amount of radioactive materials into the ocean (in the
696 vicinity of a port) as a result of the accident in the Fukushima Daiichi Nuclear Power Station (Estimation
697 made as of May 2012). Tokyo Electric Power Company. [Internet] Available from
698 (http://www.tepco.co.jp/en/press/corp-com/release/betu12_e/images/120524e0202.pdf). (Date of
699 access: 07/03/2016).

700 Trémillon, B. (1965) Les séparations par les résines échangeuses d'ions. Gauthier-Villars.

701 Utsunomiya, S., Iwata, H., Kawamoto, Y., Kaneko, M., Nakamatsu, Y., Ohnuki, T., Nanba, K. (2012)
702 Occurrence of Pu and Cs in the contaminated soils in Japan. Abstracts of Annual Meeting of the
703 Geochemical Society of Japan 59, 37.

704 Xu, C., Zhang, S., Sugiyama, Y., Ohte, N., Ho, Y.F., Fujitake, N., Kaplan, D.I., Yeager, C.M., Schwehr, K.,
705 Santschi, P.H. (2016) Role of natural organic matter on iodine and Pu distribution and mobility in
706 environmental samples from the northwestern Fukushima Prefecture, Japan. *Journal of Environmental*
707 *Radioactivity* 153, 156-166.

708 Yamamoto, M., Sakaguchi, A., Ochiai, S., Takada, T., Hamataka, K., Murakami, T., Nagao, S. (2014)
709 Isotopic Pu, Am and Cm signatures in environmental samples contaminated by the Fukushima Dai-ichi
710 Nuclear Power Plant accident. *Journal of Environmental Radioactivity* 132, 31-46.

711 Yamashiki, Y., Onda, Y., Smith, H.G., Blake, W.H., Wakahara, T., Igarashi, Y., Matsuura, Y., Yoshimura, K.
712 (2014) Initial flux of sediment-associated radiocesium to the ocean from the largest river impacted by
713 Fukushima Daiichi Nuclear Power Plant. *Scientific Reports* 4, 3714.

714 Yang, G., Zheng, J., Tagami, K., Uchida, S. (2015) Plutonium concentration and isotopic ratio in soil
715 samples from central-eastern Japan collected around the 1970s. *Scientific Reports* 5, 9636.

716 Yoshimura, C., Omura, T., Furumai, H., Tockner, K. (2005) Present state of rivers and streams in Japan.
717 *River Research and Applications* 21, 93-112.

718 Zhang, Y., Zheng, J., Yamada, M., Wu, F., Igarashi, Y., Hirose, K. (2010) Characterization of Pu
719 concentration and its isotopic composition in a reference fallout material. *Science of The Total*
720 *Environment* 408, 1139-1144.

721 Zheng, J., Aono, T., Uchida, S., Zhang, J., Honda, M.C. (2012a) Distribution of Pu isotopes in marine
722 sediments in the Pacific 30 km off Fukushima after the Fukushima Daiichi nuclear power plant accident.
723 *Geochemical Journal* 46, 361-369.

724 Zheng, J., Tagami, K., Uchida, S. (2013) Release of plutonium isotopes into the environment from the
725 Fukushima Daiichi Nuclear Power Plant accident: what is known and what needs to be known.
726 *Environmental Science & Technology* 47, 9584-9595.

727 Zheng, J., Tagami, K., Watanabe, Y., Uchida, S., Aono, T., Ishii, N., Yoshida, S., Kubota, Y., Fuma, S., Ihara,
728 S. (2012b) Isotopic evidence of plutonium release into the environment from the Fukushima DNPP
729 accident. *Scientific Reports* 2, 304.

730